OPEN ACCESS

Original research

Hepatic Krüppel-like factor 16 (KLF16) targets PPARα to improve steatohepatitis and insulin resistance

Nannan Sun,[1] Chuangpeng Shen,[2] Lei Zhang,[3] Xiaojie Wu,[4] Yuanyuan Yu,[5] Xiaoying Yang,[6] Chen Yang,[7] Chong Zhong,[8] Zhao Gao,[9] Wei Miao,[1] Zehong Yang,[1] Weihang Gao,[1] Ling Hu,[1] Kevin Williams,[10] Changhui Liu,[11] Yongsheng Chang,[3] Yong Gao [1,10]

► Additional material is published online only. To view, please visit the journal online (http://dx.doi.org/10.1136/gutjnl-2020-321774).

For numbered affiliations see end of article.

Correspondence to
Professor Yong Gao, Science and Technology Innovation Center, Guangzhou University of Chinese Medicine, Guangzhou 510006, China; profgaoyong@163.com, Professor Yongsheng Chang, Department of Physiology and Pathophysiology, Tianjin Medical University, Tianjin, China; changys@tmu.edu.cn and Dr Changhui Liu, School of Pharmaceutical Sciences, Guangzhou University of Chinese Medicine, Guangzhou, China; liuchanghui@gzucm.edu.cn

NS, CS, LZ, XW, YY, XY and CY are joint first authors.
CL, YC and YG are joint senior authors.

Received 10 May 2020
Revised 20 October 2020
Accepted 8 November 2020
Published Online First 30 November 2020

To cite: Sun N, Shen C, Zhang L, *et al*. *Gut* 2021;**70**:2183–2195.

ABSTRACT

Objective Impaired hepatic fatty acids oxidation results in lipid accumulation and redox imbalance, promoting the development of fatty liver diseases and insulin resistance. However, the underlying pathogenic mechanism is poorly understood. Krüppel-like factor 16 (KLF16) is a transcription factor that abounds in liver. We explored whether and by what mechanisms KLF16 affects hepatic lipid catabolism to improve hepatosteatosis and insulin resistance.

Design KLF16 expression was determined in patients with non-alcoholic fatty liver disease (NAFLD) and mice models. The role of KLF16 in the regulation of lipid metabolism was investigated using hepatocyte-specific KLF16-deficient mice fed a high-fat diet (HFD) or using an adenovirus/adeno-associated virus to alter KLF16 expression in mouse primary hepatocytes (MPHs) and in vivo livers. RNA-seq, luciferase reporter gene assay and ChIP analysis served to explore the molecular mechanisms involved.

Results KLF16 expression was decreased in patients with NAFLD, mice models and oleic acid and palmitic acid (OA and PA) cochallenged hepatocytes. Hepatic KLF16 knockout impaired fatty acid oxidation, aggravated mitochondrial stress, ROS burden, advancing hepatic steatosis and insulin resistance. Conversely, KLF16 overexpression reduced lipid deposition and improved insulin resistance via directly binding the promoter of peroxisome proliferator-activated receptor α (PPARα) to accelerate fatty acids oxidation and attenuate mitochondrial stress, oxidative stress in *db/db* and HFD mice. PPARα deficiency diminished the KLF16-evoked protective effects against lipid deposition in MPHs. Hepatic-specific PPARα overexpression effectively rescued KLF16 deficiency-induced hepatic steatosis, altered redox balance and insulin resistance.

Conclusions These findings prove that a direct KLF16–PPARα pathway closely links hepatic lipid homeostasis and redox balance, whose dysfunction promotes insulin resistance and hepatic steatosis.

Significance of this study

What is already known on this subject?

- Hepatic steatosis, which stems from a lipid metabolism disorder and is characterised by a dysfunction of hepatic fatty acids oxidation causing excessive ectopic lipid deposition and an altered intracellular redox balance, represents the greatest risk factor of non-alcoholic fatty liver disease (NAFLD) and insulin resistance in mammals.
- However, the details of the underlying molecular mechanisms are still unclear, and consequently, the therapeutic approach to it remains inadequate.
- In the liver, Krüppel-like factor 16 (KLF16) is an abundant transcription factor that is involved in antitumorigenicity and endocrine homeostasis. However, the function of KLF16 on hepatic lipid metabolism and insulin resistance is still undefined.

INTRODUCTION

A well-coordinated lipid metabolism, including fatty acid oxidation, lipogenesis, and lipoprotein uptake and secretion, keeps mammals in healthy conditions.[1] The ectopic overaccumulation of fatty acids drives the development of highly prevalent metabolic diseases, like hyperlipidaemia, diabetes and non-alcoholic fatty liver disease (NAFLD).[2] Approximately 15%–80% of normal and obese individuals display early manifestations of hepatic steatosis due to a high-fat diet (HFD) or an excessive alcohol intake.[3] Although a severely impaired energy homeostasis, inflammation and redox balance associate with liver steatosis progression, the underlying causative mechanisms of a progressively worsening NAFLD remain incompletely understood.

In patients with NAFLD, an impaired fatty acid oxidation is characterised by an inordinate deposition of triglycerides (TGs) inside the hepatocytes. The subsequent onset of insulin resistance, inflammation and oxidative stress aggravate NAFLD phenotype and drive the progress to non-alcoholic steatohepatitis, fibrosis, cirrhosis and even hepatocellular carcinoma.[4 5] Thus, restoration of fatty acid oxidation was proposed as an effective strategy to protect against NAFLD.[6] The transcriptional factor peroxisome proliferator-activated receptor α (PPARα) is a predominant regulator of hepatic lipid homeostasis. Under physiological conditions, PPARα pharmacological or genetic activation increased the expression of genes involved in mitochondrial and microsomal

Significance of this study

What are the new findings?

- Interestingly, hepatic KLF16 expression is significantly reduced in NAFLD patients and mice models, and the reduction of KLF16 is causatively linked to the suppression of genes involved in fatty acids oxidation and hepatic steatosis development.
- The hepatocytes-specific KLF16 knockout mice promptly develops liver steatosis and insulin resistance, due to a dysfunctional lipid catabolism. KLF16 deficiency leads to severe mitochondrial stress, redox imbalance and inflammation.
- Conversely, hepatic-specific KLF16 overexpression effectively attenuates hepatic steatosis and insulin resistance while improving hepatic mitochondrial function and mitigating both reactive oxygen species burden and inflammatory stress in HFD mice and *db/db* mice.
- KLF16 impacts on cellular lipid catabolism by directly binding to the GGGGCCCG element mapped in the peroxisome proliferator-activated receptor α (PPARα) gene promoter (from −435bp to −426bp) and activating PPARα gene transcription. Restoration of PPARα expression does recover from hepatic steatosis and insulin resistance evoked by a KLF16 deficiency.

How might it impact on clinical practice in the foreseeable future?

- Impaired fatty acid oxidation acts as a predominant risk factor of hepatic fat accumulation and insulin resistance. Our present findings prove the crucial importance of KLF16 in promoting hepatic lipid catabolism and insulin sensitivity in a PPARα-dependent manner. Targeting the KLF16–PPARα pathway supplies the molecular evidence of a novel therapeutic approach to the treatment of NAFLD.

fatty acid oxidation, facilitating gluconeogenesis and acetyl-CoA synthesis to provide the needed ATP and nicotinamide adenine dinucleotide phosphate.[7] Persistent PPARα activators could promote liver peroxisomal and mitochondrial fatty acid oxidation and have been used to treat NAFLD in clinical settings.[8–10] Conversely, PPARα deficiency led to mitochondrial dysfunction and predisposed mice to hyperketonaemia and hyperglycaemic symptoms.[11] PPARα knockout mice displayed a pronounced reactive oxygen species (ROS) generation when fed on HFD.[12] Therefore, targeting PPARα may be an effective therapeutic strategy for NAFLD.

Krüppel-like factor 16 (KLF16), consisting of Cys2/His2 zinc-finger DNA-binding proteins, belongs to a family of transcription factors rich in GT-binding or GC-binding sites. KLF16 coordinates multiple biological processes including growth, cell metabolism and cell death.[13 14] As a critical member of KLF family, KLF16 possesses a shared basic transcription element binding protein KLF group and associates with reproductive endocrinology by silencing specificity protein (Sp)/KLF sites.[15] However, hitherto, the role of KLF16 in hepatic lipid metabolism and insulin response had not been investigated.

MATERIALS AND METHODS

Patient tissue preparation

Liver samples were taken from 66 patients with biopsy for cholecystitis and preoperative testing at the First Affiliated Hospital of Guangzhou University of Chinese Medicine. Written informed consent was obtained from each patient included in the study. Viral and alcoholic hepatitis were ruled out in this study. None of the patients were treated with a lipid/glucose-lowering therapy. Samples were divided into normal group and NAFLD group based on gold-standard histological classification (NAFLD activity score (NAS)) and liver pathology.

Tolerance test

Mice were intraperitoneal injection (i.p.) injected with D-glucose (1–2 g/kg) or pyruvate sodium (1–1.5 g/kg) after 16-hour fasting. For the insulin tolerance test, mice were i.p. injected with insulin (0.5–0.75 U/kg) after 6-hour fasting. Blood glucose levels were measured respectively from the tail vein using a glucose monitor (OneTouch Ultra; On Call EZII, China) at 0, 15, 30, 45, 60, 90 and 120 min.

Cell culture

Mouse primary hepatocytes (MPHs) were isolated from livers of male C57BL/6J mice, PPARα$^{-/-}$ mice or Klf16$^{alb-/-}$ mice (8 weeks old) as previously reported. Briefly, liver cells were isolated by injection of 0.5 mg/mL type collagenase (Sigma) through the inferior vena cava after anaesthesia in mice. Trypan blue dyes were used to detect cell activity (70% or more). Then, MPHs were cultured in RPMI-1640 Medium containing 10% fetal bovine serun (FBS), 100 units/mL penicillin and 0.1 mg/mL streptomycin. MPHs were infected with Ad-Gfp, Ad-Klf16, Ad-shLuci, Ad-shKlf16 or Ad-Pparα for 24 hours, and the medium was replaced with oleic acid and palmitic acid (OA and PA) containing fresh medium for another 24 hours. To inhibit PPARα, MPHs were treated with GW6471 (10 μM, MedChemExpress). Cells were then collected for further analysis.

Chromatin immunoprecipitation (ChIP) assay

Liver samples from indicated mice were lysised and collected. The ChIP assay were done using EZ ChIP Chromatin Immunoprecipitation Kit (Cell Signaling Technology, Danvers, USA), following the manufacturer's instructions. The protein–DNA complexes were immunoprecipitated with mouse IgG antibody (control) or anti-KLF16 antibody. The promoter region of PPARα was amplified by PCR and qPCR, using primers: F:CACTGCCGTCCAGGGGGTGT; R:CCCTGCGGGGTCCCGCGGCG.

Fatty acid oxidation assays

Adenovirus-infected MPHs were incubated with 0.4 μCi/mL [9,10-^{3} H] oleic acid (PerkinElmer Life Science) and 100 μM unlabelled oleic acid (conjugated with bovine serum albumin (BSA)) in Krebs-Ringer buffer (119 mM NaCl, 5 mM KCl, 2 mM $CaCl_2$, 2.6 mM $MgSO_4$, 24.6 mM $NaHCO_3$, 2.6 mM KH_2PO_4, 10 mM HEPES, pH 7.4) for 1 hour at 37°C. Supernatants were collected and incubated with 1.3 M perchloric acid. All samples were next centrifuged at 16 000× g for 10 min. Supernatants were neutralised with 2 M KOH, 0.6M MOPS. Scintillation liquid (3 mL) was then added, and [^{3}H] radioactivity was measured.

ROS detection

MPHs, seeded in six-well plates and treated as previously, were incubated with DCFH-DA (5 μM) at 37°C for 0.5 hour, avoiding light. Cells were rinsed thrice with PBS, and fluorescence emission was detected using fluorescence microscopy. For hepatic ROS analysis, mice were injected with DCFH-DA (10 mM) via tail vein 1 hour before sacrifice, and next their livers were

collected. ROS levels were assessed using Berthold Technologies LB983 NC100.

Transmission electron microscopy

Fresh livers (1 mm^3) or MPHs were collected and fixed for longer than 2 hours in 2% paraformaldehyde and 2.5% glutaraldehyde solution and next rinsed thrice with 0.1 M PBS. The specimens were fixed in 1% osmic acid, dehydrated first through an acetone gradient (50%, 70% and 90%), next thrice in 100% acetone and finally soaked and embedded in Epon 812 epoxy resin. Semithin sections were cut in a Reichert ultramicrotome, and next block laser positioning was performed. Ultrathin sections were stained with lead citrate and uranium acetate. The ultrastructural morphological features of hepatocytes and mitochondria were assessed under a transmission electron microscope.

Analytical procedures and chemicals

Serum concentrations of TGs, total cholesterol (TC), alanine aminotransferase (ALT) and aspartate aminotransaminase (AST) were determined using an automated Monarch device (Science and Technology Park, Guangzhou, China). Hepatic TGs and cholesterol were determined using a colorimetric diagnostic kit (Applygen Technologies, Inc, Beijing, China). Serum insulin concentrations were measured by ELISA (Mercodia, Uppsala, Sweden). Serum ketone body were determined by ELISA (R&D Systems, Minneapolis, USA). Penicillin, streptomycin, OA, PA and dimethyl sulfoxide (DMSO) were purchased from Sigma.

Statistical analysis

All results are given as means±SEMs. PRISM software (V.7.00, GraphPad Software, Inc) was used to assess statistical significance between two groups via Student's t-test and one-way analysis of variance (ANOVA) followed by post hoc Tukey test for multiple groups comparisons. The curves of body weight and tolerance tests were analysed using a repeated measure two-way ANOVA. A p value <0.05 was considered as significant.

Additional methods

Other methods are detailed in online supplementary materials and methods.

RESULTS

Hepatic KLF16 expression is decreased in hepatic steatosis

To assess genes involved in hepatic steatosis, we performed mRNA assays on livers of wild type mice fed on chow diet and HFD, as well as *db/m* and *db/db* mice. Interestingly, KLF16 expression dramatically decreased in *db/db* and HFD mice (figure 1A and B), and a fasting and refeeding cycle, which stimulates lipid dynamics, significantly changed KLF16 expression (figure 1B and online supplemental figure 1A). Consistent with this finding, KLF16 protein levels were lower in patients with NAFLD than in controls, and an OA and PA cochallenge significantly reduced KLF16 expression in MPHs and HepG2 cells (figure 1C and online supplemental figure1B,C). Immunofluorescence analysis confirmed the decreased nuclear KLF16

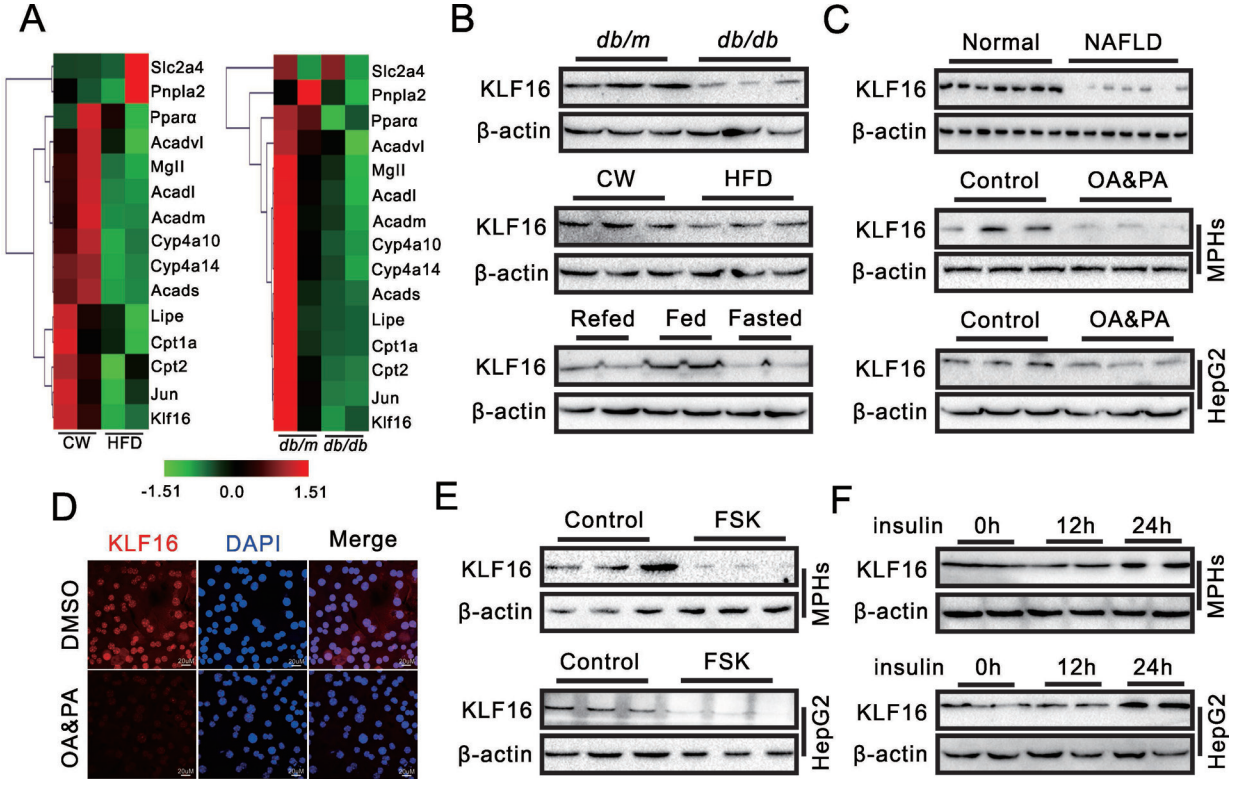

Figure 1 Hepatic KLF16 expression is downregulated in hepatic steatosis. (A) Heat map showing the expression of hepatic KLF16 and other genes regulating lipid metabolism in C57BL/6J, HFD, *db/m* and *db/db* mice (n=2/group). (B) Western blots of hepatic KLF16 in *db/db* (upper panel), HFD (middle panel) mice and C57BL/6J mice on fed and refeeding cycles (down panel) (n=6/group). (C) Western blots of KLF16 in liver samples from healthy volunteers and NAFLD patients, HepG2 cells and MPHs treated with OA and PA for 24 hours (n=6/group). (D) OA and PA treatment reduced nuclear KLF16 levels in MPHs. (E and F) FSK (E) and insulin (F) treatment changed KLF16 expression in HepG2 cells and MPHs (n=6/group). Comparable results obtained in three independent experiments. FSK, forskolin; HFD, high-fat diet; KLF16, Krüppel-like factor 16; MPH, mouse primary hepatocyte; NAFLD, non-alcoholic fatty liver disease; OA, oleic acid; PA, palmitic acid.

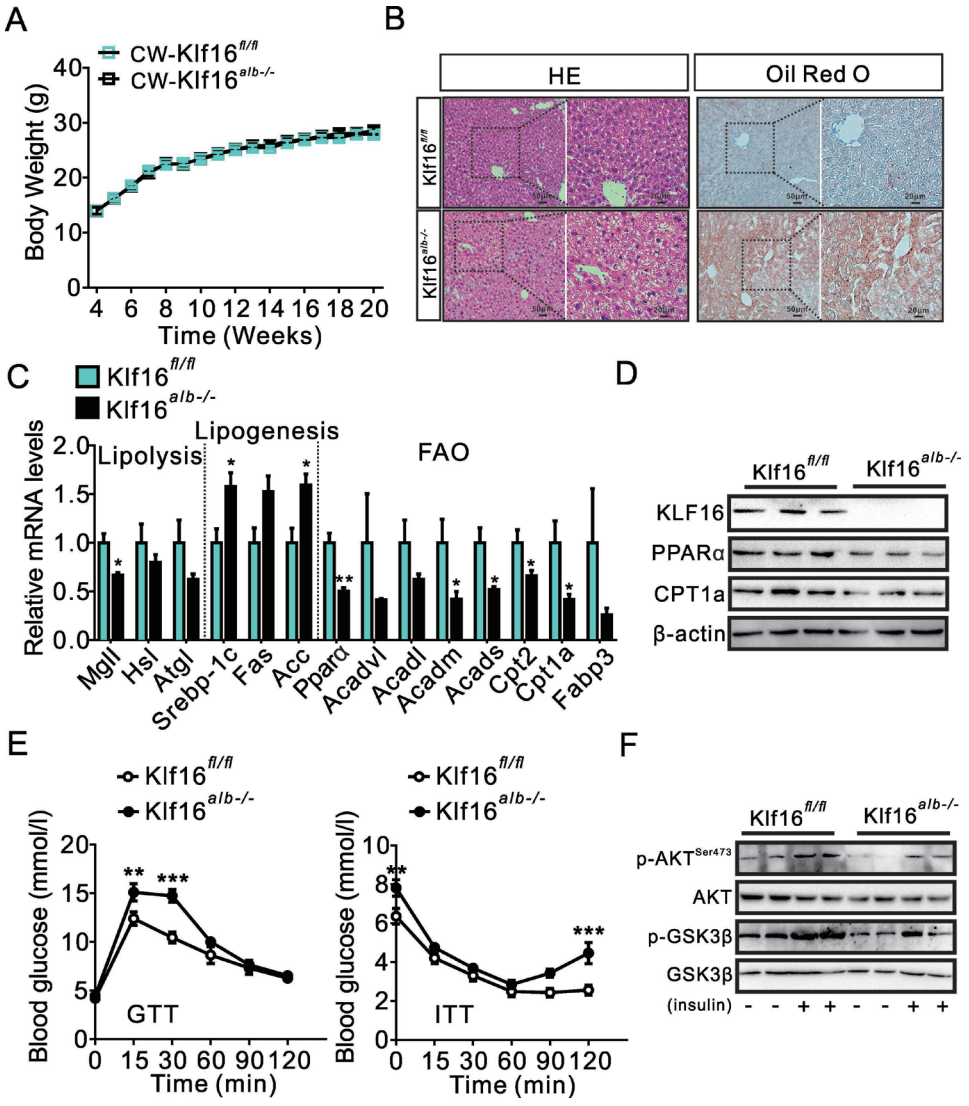

Figure 2 Hepatic KLF16 deficiency impairs lipid catabolism and insulin sensitivity. (A) Hepatic KLF16 deletion does not affect the body weight of mice on a chow diet; repeated measure two-way analysis of variance (ANOVA) was used to analyse the difference of two curves. (B) H&E and Oil red O staining increased lipid deposition in KLF16$^{alb-/-}$ mice. (C) KLF16 deletion changed the expression of genes involved in lipid metabolism. (D) KLF16 deletion reduced PPARα and CPT1A protein levels. (E) KLF16 deletion impaired glucose tolerance and insulin sensitivity; repeated measure two-way ANOVA was used to analyse the difference of two curves. (F) KLF16 deletion reduced phosphorylation of Akt/GSK-3β. Comparable results obtained in three independent experiments. Data are means±SEM; n=8 mice/group. *P<0.05, **p<0.01, ***p<0.001. KLF16,n Krüppel-like factor 16.

protein in MPHs on OA and PA treatment (figure 1D). Moreover, forskolin treatment decreased KLF16 expression in MPHs and HepG2 cells, while the presence of insulin increased KLF16 levels, implying a key ability of KLF16 to sense these hormones (figure 1E,F).

Hepatic KLF16 deficiency worsens hepatic steatosis and increases insulin resistance

To investigate the effects of KLF16 on hepatic steatosis and related metabolic disorders, we generated hepatic-specific KLF16 knockout mice (KLF16$^{alb-/-}$) (online supplemental figure 2A). Hepatic KLF16 deletion did not alter the body weight of mice on chow diet, while the ratio value of liver weight/body weight was increased (figure 2A and online supplemental figure 2B). In keeping with this, serum and hepatic TGs were increased in KLF16$^{alb-/-}$ mice, while H&E and Oil red O staining also demonstrated the occurrence of a severe lipid accumulation in the same mice (figure 2B and online supplemental figure 2C). Conversely, TC content was not affected (online supplemental figure 2C). Moreover, we found that KLF16 deficit significantly increased the expression of genes involved in fatty acid synthesis and suppressed the genes involved in lipolysis and fatty acids oxidation, especially PPARα and its target genes (figure 2C,D).

Interestingly, hepatic KLF16 deletion also increased fasting blood glucose and insulin levels (online supplemental figure 2D). KLF16 deficit impaired glucose tolerance, pyruvate tolerance and insulin sensitivity and went along with an elevated expression of gluconeogenesis-related genes (*PEPCK* and *G6Pase*) (figure 2E and online supplemental figure 2E,F). Moreover, western immunoblotting analyses revealed a decrease in the phosphorylation of AKT and GSK3β, suggesting that insulin signalling was deeply hampered in KLF16$^{alb-/-}$ mice (figure 2F).

Additionally, the dysfunction of lipid metabolism impaired hepatic mitochondrial homeostasis in KLF16$^{alb-/-}$ mice, as revealed by decreased mitochondrial numbers and altered mitochondrial ultrastructure (online supplemental figure 2G,H).

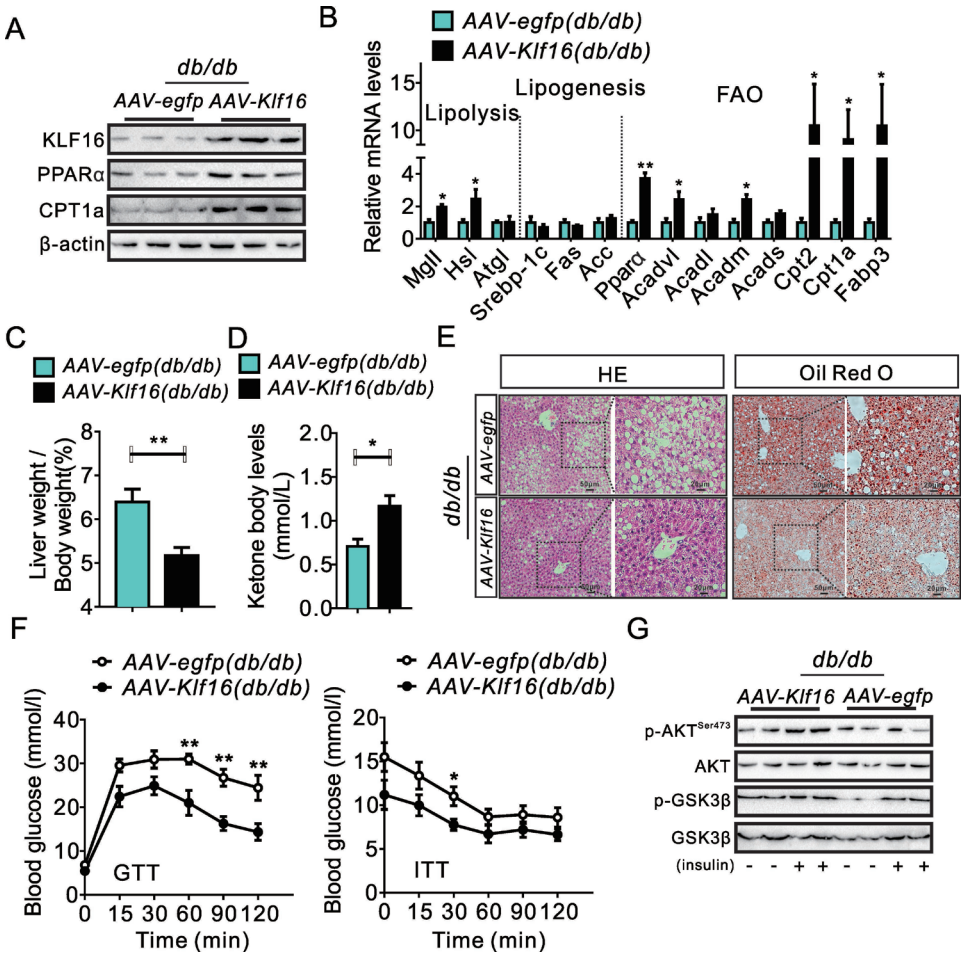

Figure 3 KLF16 overexpression alleviates hepatic steatosis in *db/db* mice. (A) KLF16 overexpression increased hepatic PPARα and CPT1A protein levels in *db/db* mice. (B) KLF16 overexpression changed the expression of genes involved in hepatic lipid metabolism in *db/db* mice. (C and D) KLF16 overexpression reduced the value of the ratio liver weight/body weight (C) and increased serum ketone body levels (D) in *db/db* mice. (E) H&E and Oil red O staining demonstrated a decreased hepatic lipid accumulation in AAV-Klf16-infected *db/db* mice. (F) KLF16 overexpression improved glucose tolerance and insulin sensitivity in *db/db* mice, repeated measure two-way analysis of variance was used to analyse the difference of two curves. (G) KLF16 overexpression increased the phosphorylation of Akt/GSK-3β in *db/db* mice. Comparable results obtained in three independent experiments. Data are means±SEM; n=8 mice/group. *P<0.05, **p<0.01. KLF16, Krüppel-like factor 16; PPARα, peroxisome proliferator-activated receptor α.

These results in a decrease in the expression of a cascade of genes involved in oxidative response and increases ROS production (online supplemental figure 2I,J). Moreover, the expression of hepatic inflammatory genes were upregulated due to KLF16 knockout, which promoted the development of hepatic steatosis and insulin resistance (online supplemental figure 2K). Collectively, these data showed that KLF16 deficiency impaired hepatic lipid and glucose metabolism, leading to hepatic steatosis and raised insulin resistance in mice.

KLF16 overexpression alleviates hepatic steatosis in *db/db* and HFD mice

We further set up hepatocyte-specific KLF16-overexpressing mice models through tail vein injections of AAV-Klf16 to confirm the function of hepatocyte KLF16 in hepatic steatosis and related metabolic disorders. AAV-Klf16 injection significantly increased hepatic-specific KLF16 overexpression in *db/db* mice, which coexisted with an upregulated expression of genes involved in fatty acid oxidation, while lipogenic genes expression did not change (figure 3A,B and online supplemental figure 3A). KLF16 overexpression did not alter the body weight but reduced the liver weight/body weight ratio value in *db/db* mice (figure 3C and online supplemental figure 3B). Moreover, AAV-Klf16-infected mice displayed a higher level of fatty acid oxidation, made plain by the elevated levels of circulating ketone bodies (figure 3D). This helped decrease hepatic lipid deposition in *db/db* mice and also reduced TGs levels, while TC level did not change (figure 3E and online supplemental figure 3C).

Moreover, KLF16 overexpression effectively decreased fasting blood glucose and insulin levels (online supplemental figure 3D). Thus, KLF17 overexpression in hepatocytes improved glucose tolerance, pyruvate tolerance and insulin sensitivity in *db/db* mice and helped suppress gluconeogenesis-related genes and recovered of insulin signalling (figure 3F,G and online supplemental figure 3E,F).

In parallel, KLF16 overexpression improved hepatic function in *db/db* mice, as shown by the decreased levels of ALT and AST (online supplemental figure 3G). Also, electron microscopy pictures of hepatic tissue confirmed the improved mitochondrial biogenesis and ultrastructural features (online supplemental figure 3H,I), both of which may have helped reduce hepatic ROS and upregulate the expression of genes involved in oxidative stress (online supplemental figure 3JK). Finally, KLF16 overexpression effectively downregulated the inflammatory genes

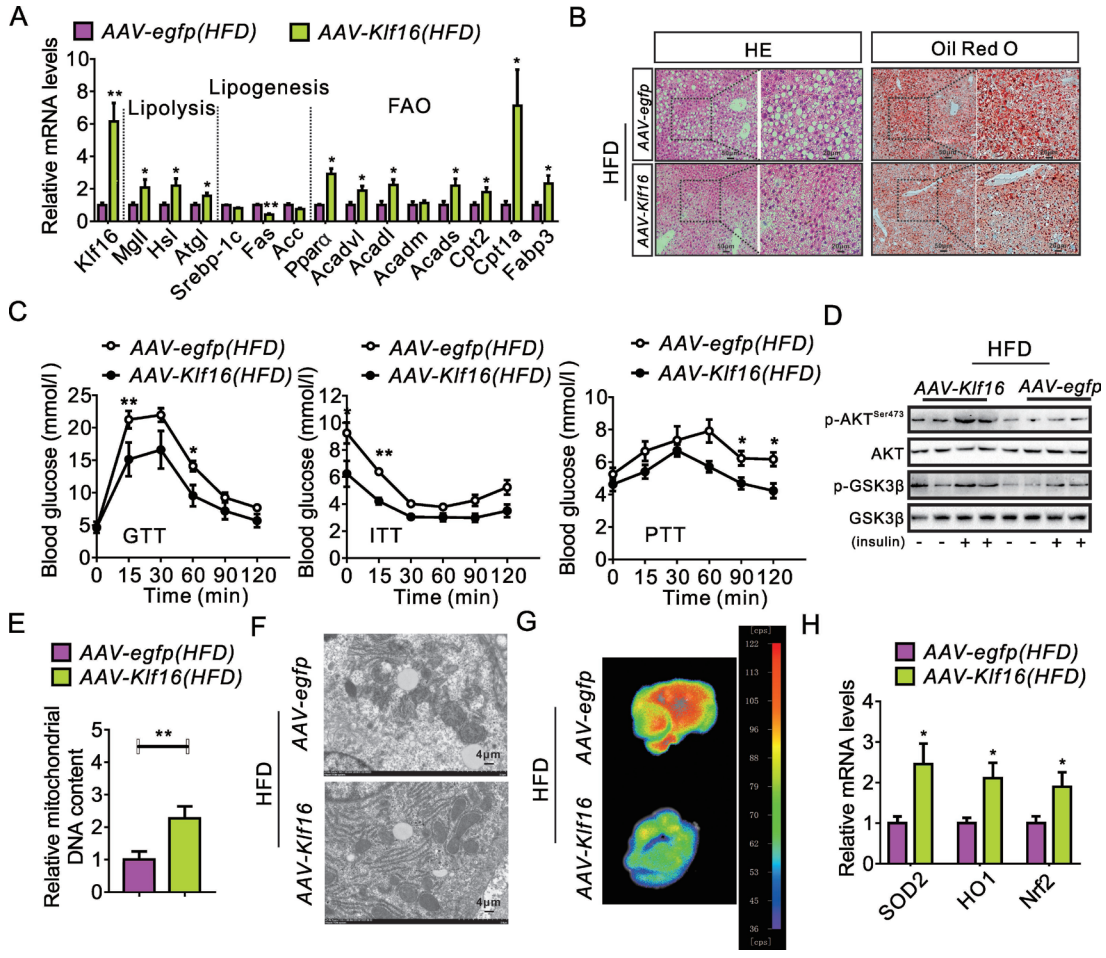

Figure 4 KLF16 overexpression improves hepatic steatosis in HFD mice. (A) KLF16 overexpression changed the expression of hepatic genes involved in lipid metabolism in HFD mice. (B) H&E and Oil red O staining demonstrated reduced lipid levels in AAV-KLF16-infected HFD mice. (C) KLF16 overexpression increased glucose tolerance and insulin sensitivity in HFD mice; repeated measure two-way analysis of variance was used to analyse the difference of two curves. (D) KLF16 overexpression increased phosphorylation of Akt/GSK-3β in HFD mice. (E and F) KLF16 overexpression promoted hepatic mitochondrial biogenesis (E) and improved the ultrastructural features (F) in HFD mice. (G and H) KLF16 overexpression both decreased HFD-induced ROS overproduction (G) and increased antioxidant genes expression (H). Equivalent results obtained in three independent experiments. Data are means±SEM; n=8 mice/group. *P<0.05, **p<0.01. HFD, high-fat diet; KLF16, Krüppel-like factor 16; ROS, reactive oxygen species.

in *db*/*db* mice, which helped attenuate liver steatosis (online supplemental figure 3L).

Corresponding results obtained in HFD mice. AAV-Klf16 infection increased hepatic-specific KLF16 expression in HFD mice and upregulated the expression of genes involved in fatty acid oxidation (figure 4A and online supplemental figure 4A). KLF16 overexpression did not change the body weight but reduced the liver weight/body weight ratio value in HFD mice (online supplemental figure 4B,C). Likewise, AAV-Klf16-infected HFD mice displayed an improved NAFLD phenotype as attested by a reduced hepatic lipid deposition and TGs levels (figure 4B and online supplemental figure 4D). Moreover, KLF16 overexpression decreased serum ALT and AST levels, suggesting an improvement of hepatic function in HFD mice (online supplemental figure 4E). Of note, AAV-Klf16-infected HFD mice exhibited decreased fasting blood glucose and insulin levels (online supplemental figure 4F). Moreover, the KLF16 overexpression significantly improved the HFD-induced glucose intolerance, pyruvate intolerance and insulin resistance, which went along with a suppression of gluconeogenesis-related genes and an upregulated insulin signalling (figure 4C,D and online supplemental figure 4G). Additionally, KLF16 overexpression also increased the numbers and improved the ultrastructural features of liver mitochondria in HFD mice (figure 4E,F). This significantly mitigated the otherwise HFD-induced hepatic ROS overproduction and altered expression of genes involved in oxidative stress (figure 4G and H). Finally, KLF16 overexpression suppressed inflammatory genes in the livers of HFD mice, helping ameliorating liver steatosis (online supplemental figure 4H).

KLF16 regulates hepatic lipid metabolism in a PPARα-dependent manner

To systemically explore the mechanism by which KLF16 affects hepatic metabolism, RNAseq data of liver samples from Ad-Klf16 infected C57BL/6J mice were analysed. They showed that 2545 genes were differently expressed with 1229 genes upregulated and 1313 gene downregulated (figure 5A). Kegg pathway analysis showed that KLF16 overexpression significantly altered hepatic fatty acid metabolism and PPAR signalling pathway (figure 5B), as it highly induced PPARα and its target

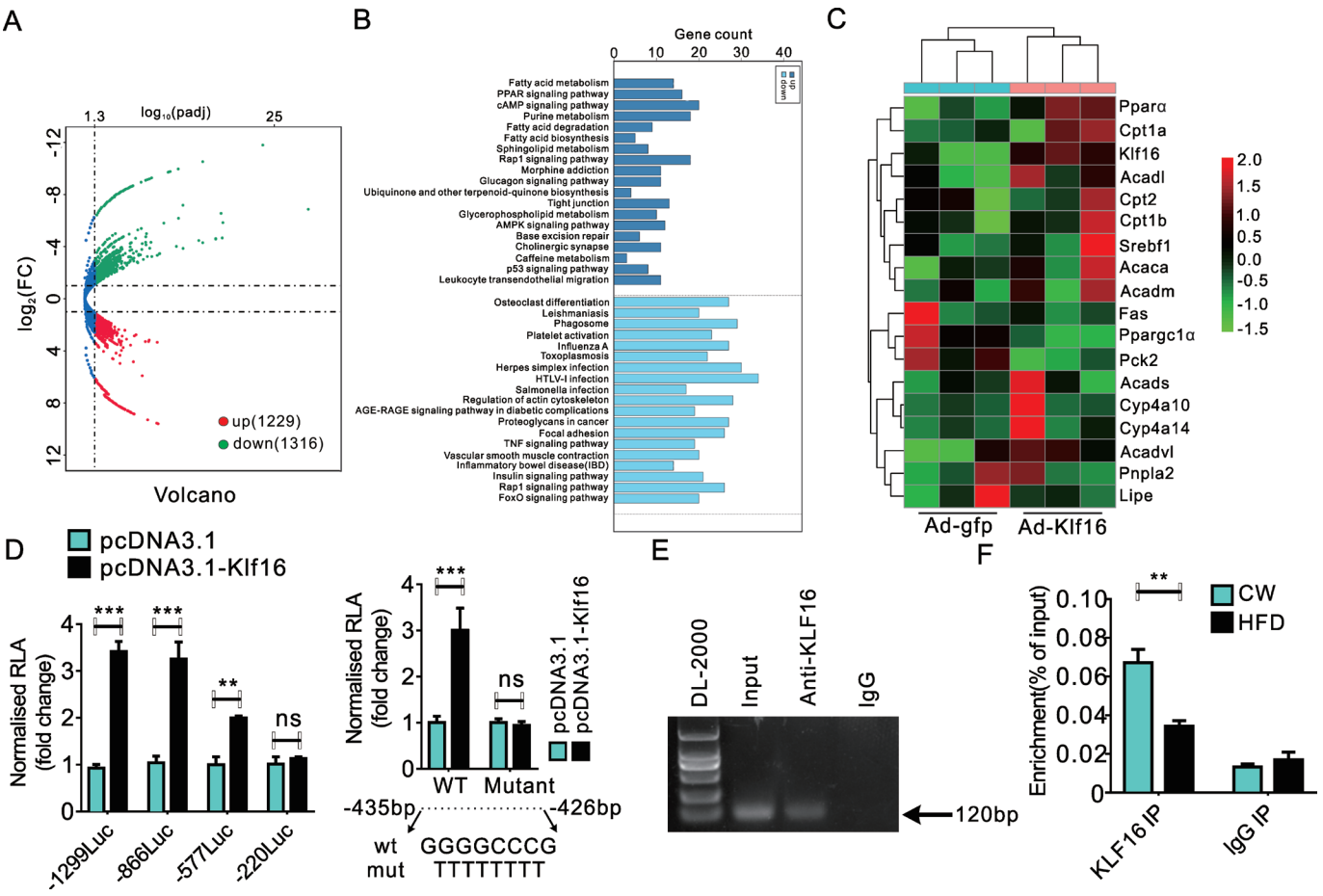

Figure 5 Via binding PPARα promoter region KLF16 affects fatty acid oxidation. (A and B) Scatter plot (A), KEGG analysis (B) and heatmap (C) of RNAseq data in Ad-Gfp-infected or Ad-Klf16-infected C57BL/6J mice showing that KLF16 affects fatty acid oxidation and the expression of PPARα and its downstream target genes. (D) Luciferase reporter gene assay demonstrated the existence of a potential KLF16 binding site from −220bp to −577bp (left) and that a mutation between −426bp and −435bp abrogates any KLF16-induced transcriptional activity (right). (E and F) ChIP (E) and ChIP-qPCR (F) assessed the endogenous KLF16 enrichment on PPARα′ promoter in the liver of mice on chow diet or HFD. Comparable results obtained in three independent experiments. Data are means±SEM; n=6/group. *P<0.05, **p<0.01, ***p<0.001. HFD, high-fat diet; KLF16, Krüppel-like factor 16; PPARα, peroxisome proliferator-activated receptor α.

genes, suggesting a potential mediation of KLF16-evoked effects by PPARα (figure 5C). We further conducted luciferase assays using reporter constructs (pPPARα−1299, pPPARα−866, pPPARα−577 and pPPARα−220) in HepG2 cells. Our results revealed that KLF16 increased the transcriptional activity of pPPARα−1299, pPPARα−866 and pPPARα−577, while the stimulatory effects disappeared when the promoter region was further truncated to −220 bp (figure 5D, *left panel*), suggesting a KLF16 binding site being located from −577bp to −221bp. Mutation of the −435/−426nt site significantly diminished the KLF16-mediated activation of PPARα (figure 5D, *right panel*). Additionally, the occupancy of KLF16 on PPARα promoter was confirmed using a ChIP assay, and our ChIP-qPCR data also revealed a decreased KLF16 enrichment of the PPARα promoter fragment in HFD mice (figure 5E,F). In MPHs, KLF16 overexpression increased fatty acids oxidation and reduced lipid deposition by upregulating PPARα and its target genes (figure 6A–C and online supplemental figure 5A). Conversely, silencing KLF16 elicited the opposite effects (figure 6D–F and online supplemental figure 5B), thereby implying a strong correlation between KLF16 function and PPARα-mediated fatty acid oxidation. To further validate the key role of PPARα to mediate the KLF16-induced protective effects, we treated wild-type MPHs with GW6471, followed by Ad-Klf16 infection and OA and PA treatment for another 24 hours. In keeping with our hypothesis, PPARα pharmacological inhibition significantly diminished the KLF16-evoked protective effects against lipid deposition, as shown by the unchanged Oil red O-stained lipid levels and cellular TGs contents (figure 6G). Very similarly, KLF16 overexpression did not alter the OA and PA induced lipid accumulation in PPARα-deficient MPHs isolated from PPARα$^{-/-}$ mice (figure 6H).

PPARα overexpression attenuated KLF16 deficiency-induced hepatic steatosis

To further confirm the importance role of PPARα in mediating KLF16-induced protective effects. MPHs isolated from KLF16$^{alb-/-}$ mice were infected with Ad-Pparα. As expected, Ad-Pparα infection induced a significant upregulation of PPARα in MPHs and livers (online supplemental figure 6A). Moreover, PPARα overexpression effectively rescued KLF16 deficit-induced lipid accumulation in MPHs (figure 7A,B).

We also injected Ad-Pparα into KLF16$^{alb-/-}$ mice fed on HFD to confirm the PPARα capability to mediate the KLF16-induced effects. Ad-Pparα infection significantly stimulated the hepatic

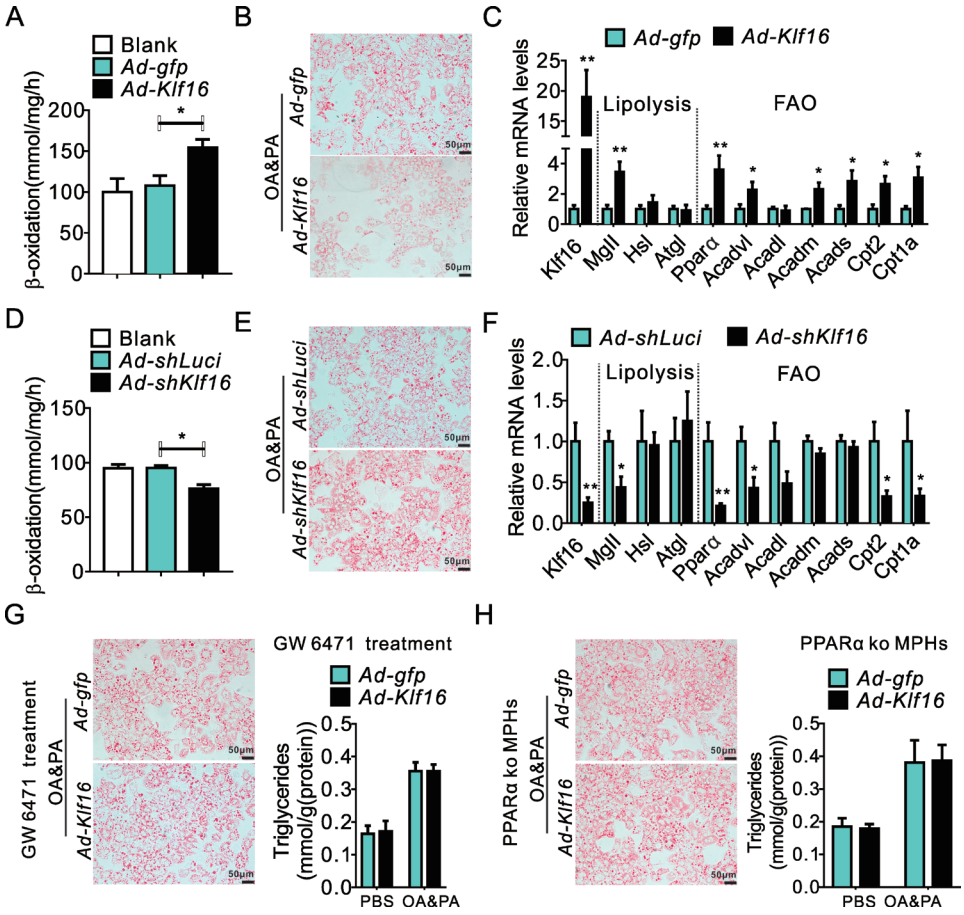

Figure 6 KLF16 regulates hepatic lipid metabolism in a PPARα-dependent manner (A–C) KLF16 overexpression increased fatty acid metabolism (A), decreased OA and PA induced lipid accumulation (B) and upregulated the genes involved in lipolysis and fatty acid oxidation (C). (D–F) KLF16 knockdown decreased fatty acid oxidation (D), worsened OA and PA induced lipid accumulation and suppressed the expression of genes involved in lipolysis and fatty acid oxidation (F). (G and H) Pharmacological inhibition or gene knockout of PPARα diminished the protective effects of KLF16 overexpression against lipid deposition. Equivalent results obtained in three independent experiments. Data are means±SEM; n=6/group. *P<0.05, **p<0.01. KLF16, Krüppel-like factor 16; MPHs, mouse primary hepatocytes; OA, oleic acid; PA, palmitic acid; PBS, phosphate buffered saline; PPARα, peroxisome proliferator-activated receptor α.

expression of PPARα and its target genes (figure 7C and online supplemental figure 6B). Ad-Pparα-infected KLF16$^{alb-/-}$ mice displayed reductions in body weight and liver weight/body weight ratio value (online supplemental figure 6C,D). Moreover, PPARα overexpression effectively decreased TGs levels and hepatic lipid accumulation in HFD KLF16$^{alb-/-}$ mice (figure 7D,E). However, hepatic TCs content only slight decreased (figure 7D). Notably, PPARα overexpression rescued HFD-induced mitochondrial dysfunction in KLF16$^{alb-/-}$ mice, as manifested by the increased numbers and improved ultrastructural features of the mitochondria (online supplemental figure 6E). These changes significantly reduced liver ROS overproduction and inflammatory genes elevation in HFD KLF16$^{alb-/-}$ mice (online supplemental figure 6F,G). PPARα overexpression effectively decreased both ALT and AST levels in KLF16$^{alb-/-}$ mice on HFD, indicating an improved hepatic function (online supplemental figure 6H). More importantly, PPARα overexpression significantly improved the glucose metabolism disorder in KLF16$^{alb-/-}$ mice fed on HFD, as shown by reductions in fasting blood glucose and insulin levels (online supplemental figure 6I). The PPARα overexpression-mediated recovery of insulin signalling improved glucose intolerance, pyruvate intolerance and decreased insulin resistance (figure 7F and G). Altogether, these data suggested that PPARα plays crucial roles in mediating the several KLF16-induced protective effects.

KLF16 maintains intracellular redox balance in a PPARα-dependent manner

Previous studies indicated that an immoderate fatty acids accumulation drives ROS overproduction and promotes NAFLD progression.[16 17] Thus, we investigated KLF16 effects on the intracellular redox system. As expected, KLF16 overexpression effectively elevated mitochondrial biogenesis and promoted mitochondrial fission in MPHs under OA and PA treatment (figure 8A,B). Moreover, KLF16 overexpression also significantly upregulated genes playing antioxidative roles, for example, *Nrf2*, *SOD2* and *HO1* (figure 8C). This led to a remarkable decrease in OA and PA elicited ROS production, thereby improving the redox balance disorder in MPHs (online supplemental figure 7A). Conversely, KLF16 deletion decreased mitochondrial numbers while increasing MPHs sensitivity to OA and PA treatment, as shown by the mitochondrial deeply altered ultrastructural features (figure 8D,E). KLF16 deficiency after OA and PA treatment resulted in ROS overproduction due to antioxidant genes suppression (figure 8F and online supplemental figure 7B). Consistent with our above findings, PPARα plays a crucial role in mediating the protective effects of KLF16 on intracellular redox imbalance. PPARα overexpression effectively ameliorated OA and PA induced ROS overproduction in KLF16-deficient MPHs while also restoring the expression

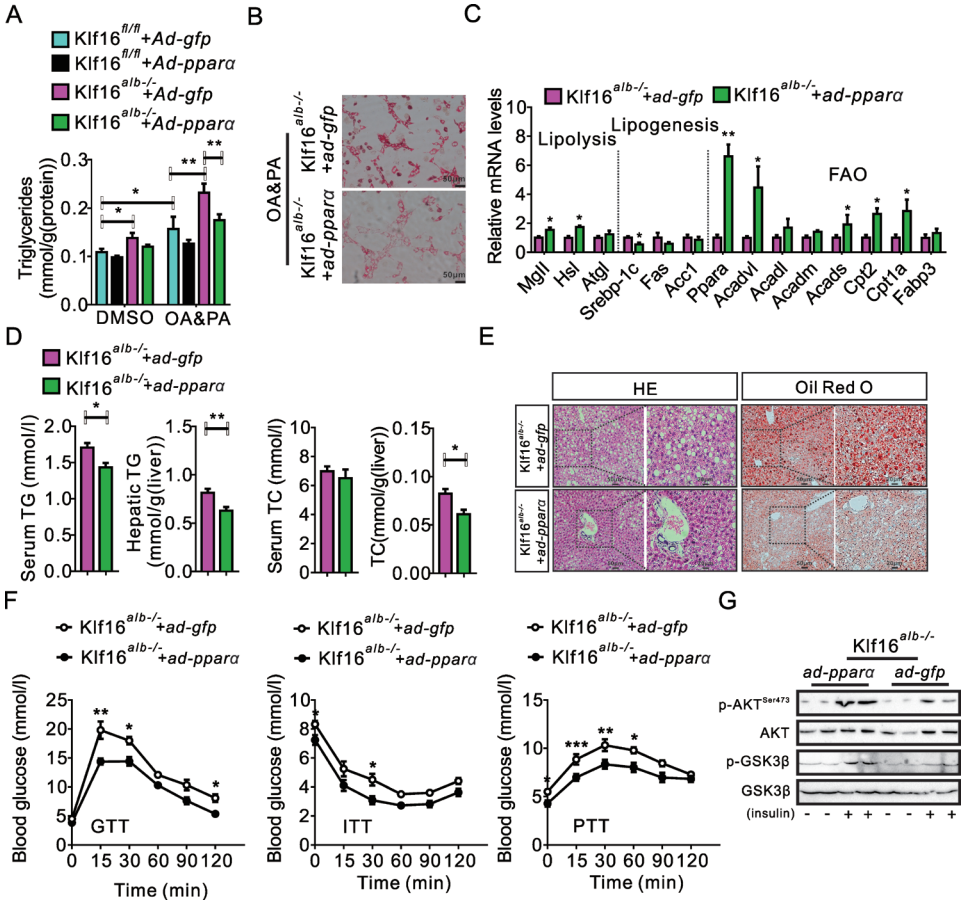

Figure 7 PPPARα overexpression mitigated KLF16 deficiency-induced hepatic steatosis. (A and BB) PPARα overexpression reduced KLF16 deficiency-intensified lipid deposition after OA and PA treatment. (C) Hepatic *PPARα* overexpression changed the activity of genes that are involved in lipid metabolism. (D) PPARα overexpression reduced serum and hepatic TGs levels, and slightly decreased hepatic TCs content in KLF16$^{alb-/-}$ mice fed on HFD. (E) Ad-Pparα infection decreased hepatic lipid deposition in HFD KLF16$^{alb-/-}$ mice. (F) Ad-Pparα infection increased glucose tolerance, insulin sensitivity and pyruvate tolerance in HFD KLF16$^{alb-/-}$ mice; repeated measure two-way analysis of variance was used to analyse the difference of two curves. (G) PPARα overexpression increased the phosphorylation of Akt/GSK-3β in HFD KLF16$^{alb-/-}$ mice. Equivalent results were obtained in three independent experiments. Data are means±SEM, n=8 mice/group. *P<0.05, **p<0.01, ***p<0.001. HFD, high-fat diet; KLF16, Krüppel-like factor 16; OA, oleic acid; PA, palmitic acid; PPARα, peroxisome proliferator-activated receptor α; TC, total cholesterol; TGs, triglycerides.

of genes involved in fatty acids oxidation (figure 8G). However, KLF16 overexpression failed to improve the OA and PA induced redox balance disorder after PPARα genetic deletion in MPHs, as revealed by the persistently heightened ROS levels (figure 8H). These data showed the existence of a KLF16–PPARα dependent cooperation keeping intracellular redox homeostasis, which affects hepatic lipid metabolism.

Hepatic KLF16 deletion increases mice sensitivity to ethanol feeding

Previous studies revealed that an impaired hepatic fatty acids oxidation also contributes to the development of alcohol-induced fatty liver, alcoholic hepatitis and cirrhosis.[18 19] Thus, we used these mice as further models to confirm the effects of the KLF16–PPARα axis on hepatic fatty acid oxidation. Interestingly, ethanol feeding significantly inhibited hepatic KLF16 expression and decreased KLF16 enrichment on the PPARα promoter (figure 9A,B and online supplemental figure 8A). KLF16$^{alb-/-}$ mice fed on ethanol displayed a severe hepatic lipid accumulation and a weightier liver (figure 9C,D). Moreover, hepatic TGs levels quickly rose in KLF16$^{alb-/-}$ mice fed on ethanol diet (figure 9E). KLF16 deletion also results in an increased of serum ALT and AST levels, along with an prompt upregulation of hepatic inflammatory genes after ethanol diet feeding (online supplemental figure 8B,C). In keeping with our previous findings, KLF16 deletion aggravated the alcohol-induced suppression of genes involved in fatty acid oxidation (figure 9F). Moreover, mitochondrial dysfunction and redox imbalance became irreversible, as shown by the grievous fusion of mitochondria and the overproduction of ROS in these mice (online supplemental figure 8D,E).

In summary, these data suggest that KLF16 directly binding PPARα promoter is essential to maintain a healthy hepatocytic intracellular environment and defend against NAFLD or alcohol-induced fatty liver disease via recovery of impaired hepatic fatty acid oxidation.

DISCUSSION

NAFLD has become the most prevalent aetiological factor of chronic liver diseases.[20] The earlier pathogenetic view about the development of NAFLD was the 'two-hit hypothesis', envisaging that concurring imbalances of hepatic lipid synthesis and oxidation cause a local surplus accumulation of fatty acids, promoting hepatic steatosis development.[21 22] Recent studies proposed the 'multiple hit hypothesis', which envisions several insults acting together on genetically predisposed subjects to induce NAFLD, thus more accurately explaining the latter's pathogenesis.[23–26]

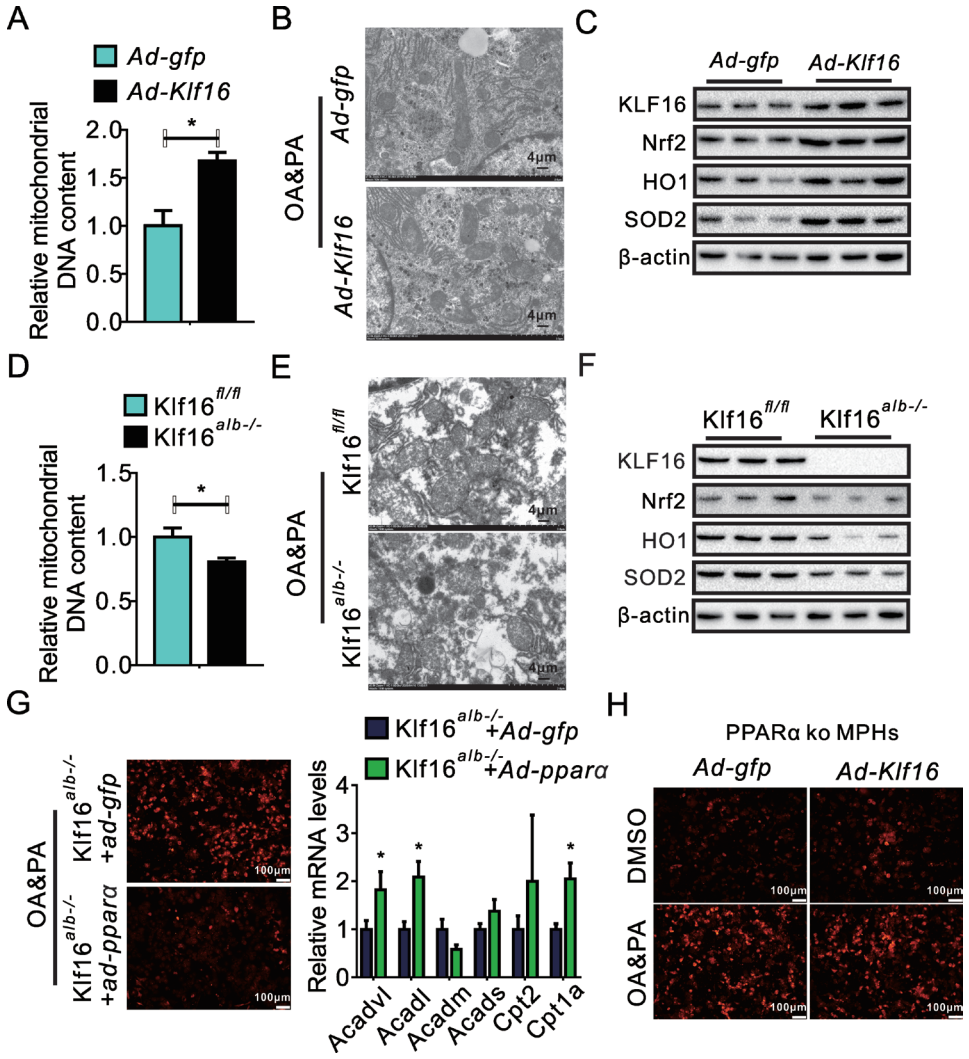

Figure 8 KLF16 maintains the intracellular redox balance in a PPARα-dependent manner. (A and B) KLF16 overexpression increased mitochondrial biogenesis (A) and improved mitochondrial ultrastructural features (B) in MPHs. (C) KLF16 overexpression increased the expression of antioxidant genes. (D and E) KLF16 deletion decreased mitochondrial biogenesis (D) and altered mitochondrial ultrastructural features (E) in MPHs. (F) KLF16 deficiency decreased the expression of antioxidant genes. (G) PPARα overexpression rescued OA and PA induced ROS overproduction (*left panel*) and the expression of the genes involved in fatty acid oxidation (*right panel*) in KLF16-deficient MPHs. (H) KLF16 overexpression failed to alter OA and PA induced ROS production in PPARα^{ko} MPHs. Comparable results obtained in three independent experiments. Data are means±SEM; n=6/group. *P<0.05. KLF16, Krüppel-like factor 16; MPHs, mouse primary hepatocytes; OA, oleic acid; PA, palmitic acid; PPARα, peroxisome proliferator-activated receptor α; ROS, reactive oxygen species.

Such hits include an increased insulin resistance, adipose tissue-secreted hormones, nutritional factors, altered gut microbiota and genetic and epigenetic factors. Despite the 'two-hit' or 'multiple hit' hypotheses, one of the key consequences of NAFLD is the inordinate lipids accumulation, such as free fatty acids, in the liver. This fact critically points to a potential therapeutic strategy for the treatment of NAFLD.

Emerging evidence have revealed lipogenesis (de novo fatty acid synthesis), fatty acid oxidation, and lipoprotein uptake and secretion tightly control hepatic lipid homeostasis.[8 27] Deregulations of lipogenesis or fatty acid oxidation cause NAFLD development. Therefore, any strategy aimed at decreasing liver's lipid load by effectively repressing the de novo fatty acid synthesis and by increasing fatty acid oxidation might represent a beneficial treatment of NAFLD. Sterol regulatory element binding protein-1 (SREBP-1c), a key transcription regulator of lipogenesis and TGs storage, is synthesised as an inactive precursor that is initially attached to the nuclear envelope and the endoplasmic reticulum membranes.[28] The activation of SREBP-1c plays a crucial role in metabolic diseases, especially NAFLD.[29] However, in this study, we found that KLF16 did not alter the protein levels of SREBP-1c in MPHs, both in cytoplasm and nucleus (online supplemental figure 9). At variance with SREBP-1c role in lipogenesis, PPARα is an important nuclear receptor involved in the regulation of fatty acid oxidation.[30–32] In current study, we reported that liver-specific KLF16 overexpression did remarkably enhance the expression of PPARα and its target genes including Acadvl and Cpt2, which intensified lipolysis and reduced hepatic lipid load, suggesting that the KLF16 overexpression-mediated reduction in hepatic lipids levels relates to the PPARα-mediated elevated hepatic lipolytic effect, rather than the SREBP-1c-mediated lipogenesis.

KLF16 is a member of Krüppel-like family of transcriptional factors (KLFs), which regulates cellular homeostasis playing roles in growth, development and programmed cell death.[33–35] We and others previously showed that KLFs strongly associated with the regulation of metabolic syndromes.[13 14 36–41] For instance, we

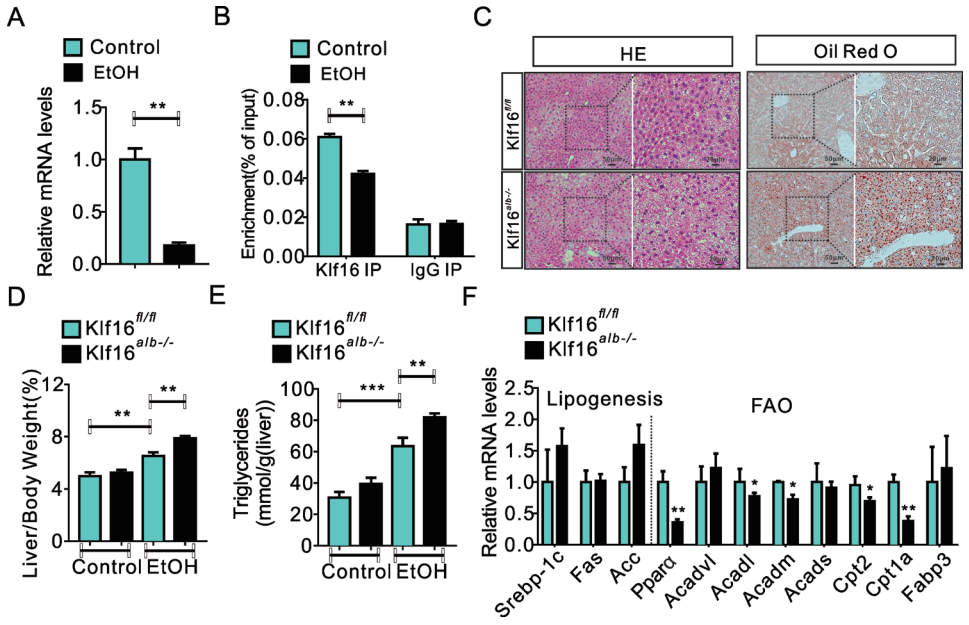

Figure 9 Hepatic KLF16 deletion renders mice more sensitive to alcohol feeding. (A and B) Ethanol feeding suppressed KLF16 expression (A) and reduced its enrichment on the PPARα promoter (B). (C) H&E and Oil red O staining demonstrated a severe hepatic lipid deposition in KLF16$^{alb-/-}$ mice fed on an ethanol diet. (Dadn E) *KLF16* deletion increased the liver weight/body weight ratio value (D) and hepatic TG content (E) during ethanol feeding. (F) KLF16 deletion suppressed the expression of genes involved in fatty acid oxidation in mice fed on an ethanol diet. Comparable results were obtained in three independent experiments. Data are means±SEM; n=8/group. *P<0.05, **p<0.01, ***p<0.001. KLF16, Krüppel-like factor 16; PPARα, peroxisome proliferator-activated receptor α; TG, triglyceride.

previously proved that mouse KLF9, KLF10 and KLF14 partake in hepatic glucose homeostasis by modulating the expression of peroxisome proliferator-activated receptor-γ coactivator-1 alpha.[13 14 36] KLF15 was identified as a pivotal component of transcriptional circuitry coordinating the physiological fluxes of three basic kinds of cellular nutrients: that is, glucose, amino acids and lipids.[37–39] We also showed that mouse KLF11 regulates hepatic lipid metabolism by targeting the PPARα signalling pathway via an unknown mechanism.[40] Recently, Bechmann *et al*[41] revealed that KLF6 is a novel regulator of glucose and lipid metabolism by mediating the PPARα post-transcriptional activation. Differently from previous reports, in this study, we offer the direct evidence that, being a transcription factors, KLF16 directly binds PPARα's promoter domain at a location placed from −577bp to −221bp endowed with GT-rich or GC-rich elements. PPARα deletion could remarkably abrogate KLF16 overexpression-mediated alleviation of OA and PA induced lipid deposition in MPHs. Conversely, liver-specific PPARα overexpression could reverse the KLF16 deficiency-induced hepatic steatosis, demonstrating that PPARα is a bona fide target gene of KLF16. In keeping with our results, KLF1 demonstrated a similar transcriptional regulatory mode.[42]

Accumulating evidence suggest that an excessive lipid deposition stimulates the intracellular production of ROS by impairing the lysosomal–mitochondrial axis.[43] Besides, chronic HFD exposure activated JNK and drove its migration into the mitochondria triggering a vicious ROS-JNK feed-forward loop resulting in oxidative stress and eventually causing hepatocytes' death. Healthy hepatocytes are endowed with systems comprising antioxidant enzymes and antioxidant genes such as PPARα, Nrf2 and Ho1, which eliminate ROS surpluses and maintain the redox balance. PPARα activation effectively protected mice against cholestasis-induced hepatic injury by inhibiting JNK signalling. A PPARα antagonist effectively inhibited liver glycogen synthase kinase-3β (GSK-3β) and p(Thr183/Tyr185)-JNK. We proved that KLF16 overexpression efficaciously improved HFD-induced or alcohol-induced hepatic mitochondrial stress and ROS overproduction and eventually benefiting the hepatotoxicity and fatty liver phenotype. Conversely, KLF16-deficient mice showed a fast and severe lipid deposition during HFD or alcohol exposure. Moreover, ROS surpluses induce DAMP molecules release and trigger an irreversible secondary inflammatory injury through an abnormal innate immune system activation.[44] KLF16 was previously reported to suppress human glioma and glioblastoma cells proliferation by targeting TFAM, implying its potential anti-inflammatoty role. Here, we show that hepatic KLF16 acts as a negative regulator of proinflammatory genes in the liver. Moreover, we also prove that KLF16 exerts a protective effect against hepatocytes apoptosis in vivo and in vitro (online supplemental figure 10).

In summary, our results reveal that KLF16 targets the PPARα gene as it directly binds to the KLF16 promoter region, thus contributing to upregulate its expression at the transcriptional level, which crucially promotes fatty acids oxidation and acts as a new target for the treatment of fatty liver and metabolic syndrome.

Author affiliations
[1]Science and Technology Innovation Center, Guangzhou University of Chinese Medicine, Guangzhou, China
[2]Department of Endocrinology, The First Affiliated Hospital of Guangzhou University of Chinese Medicine, Guangzhou, Guangdong, China
[3]Department of Physiology and Pathophysiology, Tianjin Medical University, Tianjin, China
[4]Central Lab of Binzhou People's Hospital, Central Lab of Binzhou People's Hospital, Shandong, China
[5]Artemisinin Research Center, Guangzhou University of Chinese Medicine, Guangzhou, Guangdong, China
[6]Jiangsu Key Laboratory of Immunity and Metabolism, Department of Pathogen Biology and Immunology, Xuzhou Medical University, Xuzhou, Jiangsu, China
[7]School of Pharmaceutical, Guangzhou University of Chinese Medicine, Guangzhou, Guangdong, China
[8]Department of Hepatobiliary Surgery, The First Affiliated Hospital of Guangzhou University of Chinese Medicine, Guangzhou, Guangdong, China
[9]Guangdong Provincial Institute of Sports Science, Guangzhou, Guangdong, China

[10]Division of Hypothalamic Research, University of Texas Southwestern Medical Center at Dallas, Dallas, Texas, USA
[11]School of Pharmaceutical Sciences, Guangzhou University of Chinese Medicine, Guangzhou, Guangdong, China

Acknowledgements We would like to thank Professor Hongbing Zhang and Yongsheng Chang for providing alb-cre mice and Ad-Pparα adenovirus.

Contributors YG and YC conceived the idea and designed the experiment. NS, XW, CS, LZ and CS performed experiments. CZ, CL, ZG, WM, ZY, WG, XY, YY, LH and KW analysed the data and improved the manuscript.

Funding This work was supported by the National Natural Science Foundation of China (grant nos. 81800738, 81773969, 81102883, 81800718 and 82070891), the first-class discipline construction major project of Guangzhou University of Chinese Medicine (Guangzhou University of Chinese Medicine Planning (2018, No. 6), Guangzhou University of Chinese Medicine Planning (2019, No. 5)), the Guangdong Science and Technology Collaborative Innovation Center for Sport Science (2019B110210004), the Natural Science Foundation of the Jiangsu Higher Education Institutions of China (No. 18KJB310015), the Jiangsu Shuangchuang Programme and the Starting Foundation for Talents of Xuzhou Medical University (No. D2018006). Shandong key research and development program (2019GSF108270).

Competing interests None declared.

Patient consent for publication Not required.

Ethics approval The study protocol conforms to the ethical guidelines of the 1975 Declaration of Helsinki as reflected in a priori approval by the ethics committees of the First Affiliated Hospital of Guangzhou University of Chinese Medicine (NO. K [2019]082).

Provenance and peer review Not commissioned; externally peer reviewed.

Data availability statement Data are available on reasonable request.

ORCID iD
Yong Gao http://orcid.org/0000-0003-3879-7601

REFERENCES

1 Browning JD, Horton JD. Molecular mediators of hepatic steatosis and liver injury. *J Clin Invest* 2004;114:147–52.
2 Morino K, Petersen KF, Shulman GI. Molecular mechanisms of insulin resistance in humans and their potential links with mitochondrial dysfunction. *Diabetes* 2006;55:S9–15.
3 Bellentani S. The epidemiology of non-alcoholic fatty liver disease. *Liver Int* 2017;37:81–4.
4 Diraison F, Moulin P, Beylot M. Contribution of hepatic de novo lipogenesis and reesterification of plasma non esterified fatty acids to plasma triglyceride synthesis during non-alcoholic fatty liver disease. *Diabetes Metab* 2003;29:478–85.
5 Van De Wier B, Koek GH, Bast A, *et al*. The potential of flavonoids in the treatment of non-alcoholic fatty liver disease. *Crit Rev Food Sci Nutr* 2017;57:834–55.
6 Kammoun HL, Chabanon H, Hainault I, *et al*. Grp78 expression inhibits insulin and ER stress-induced SREBP-1c activation and reduces hepatic steatosis in mice. *J Clin Invest* 2009;119:1201–15.
7 Mandard S, Müller M, Kersten S. Peroxisome proliferator-activated receptor alpha target genes. *Cell Mol Life Sci* 2004;61:393–416.
8 Rotman Y, Sanyal AJ. Current and upcoming pharmacotherapy for non-alcoholic fatty liver disease. *Gut* 2017;66:180–90.
9 Huang J, Jia Y, Fu T, *et al*. Sustained activation of PPARα by endogenous ligands increases hepatic fatty acid oxidation and prevents obesity in ob/ob mice. *Faseb J* 2012;26:628–38.
10 Li Q, Tian Z, Wang M, *et al*. Luteoloside attenuates neuroinflammation in focal cerebral ischemia in rats via regulation of the PPARγ/Nrf2/NF-κB signaling pathway. *Int Immunopharmacol* 2019;66:309–16.
11 Leone TC, Weinheimer CJ, Kelly DP. A critical role for the peroxisome proliferator-activated receptor alpha (PPARalpha) in the cellular fasting response: the PPARalpha-null mouse as a model of fatty acid oxidation disorders. *Proc Natl Acad Sci U S A* 1999;96:7473–8.
12 Pawlak M, Baugé E, Lalloyer F, *et al*. Ketone body therapy protects from lipotoxicity and acute liver failure upon PPARα deficiency. *Mol Endocrinol* 2015;29:1134–43.
13 Cui A, Fan H, Zhang Y, *et al*. Dexamethasone-induced Krüppel-like factor 9 expression promotes hepatic gluconeogenesis and hyperglycemia. *J Clin Invest* 2019;129:2266–78.
14 Yang X, Chen Q, Sun L, *et al*. Klf10 transcription factor regulates hepatic glucose metabolism in mice. *Diabetologia* 2017;60:2443–52.
15 Daftary GS, Lomberk GA, Buttar NS, *et al*. Detailed structural-functional analysis of the Krüppel-like factor 16 (KLF16) transcription factor reveals novel mechanisms for silencing Sp/KLF sites involved in metabolism and endocrinology. *J Biol Chem* 2012;287:7010–25.
16 Fang Y-L, Chen H, Wang C-L, *et al*. Pathogenesis of non-alcoholic fatty liver disease in children and adolescence: From "two hit theory" to "multiple hit model". *World J Gastroenterol* 2018;24:2974–83.
17 Antonucci L, Porcu C, Iannucci G, *et al*. Non-alcoholic fatty liver disease and nutritional implications: special focus on copper. *Nutrients* 2017;9. doi:10.3390/nu9101137. [Epub ahead of print: 18 Oct 2017].
18 Zhang D, Tong X, Nelson BB, *et al*. The hepatic BMAL1/AKT/lipogenesis axis protects against alcoholic liver disease in mice via promoting PPARα pathway. *Hepatology* 2018;68:883–96.
19 Kang X, Zhong W, Liu J, *et al*. Zinc supplementation reverses alcohol-induced steatosis in mice through reactivating hepatocyte nuclear factor-4alpha and peroxisome proliferator-activated receptor-alpha. *Hepatology* 2009;50:1241–50.
20 Yeh MM, Brunt EM. Pathology of nonalcoholic fatty liver disease. *Am J Clin Pathol* 2007;128:837–47.
21 Khan RS, Bril F, Cusi K, *et al*. Modulation of insulin resistance in nonalcoholic fatty liver disease. *Hepatology* 2019;70:711–24.
22 Zhan Y-T, An W. Roles of liver innate immune cells in nonalcoholic fatty liver disease. *World J Gastroenterol* 2010;16:4652–60.
23 Buzzetti E, Pinzani M, Tsochatzis EA. The multiple-hit pathogenesis of non-alcoholic fatty liver disease (NAFLD). *Metabolism* 2016;65:1038–48.
24 Wahlang B, Jin J, Beier JI, *et al*. Mechanisms of environmental contributions to fatty liver disease. *Curr Environ Health Rep* 2019;6:80–94.
25 Poeta M, Pierri L, Vajro P. Gut-Liver axis derangement in non-alcoholic fatty liver disease. *Children* 2017;4. doi:10.3390/children4080066. [Epub ahead of print: 02 Aug 2017].
26 Tilg H, Adolph TE, Moschen AR. Multiple parallel hits hypothesis in NAFLD - revisited after a decade. *Hepatology* 2020. doi:10.1002/hep.31518. [Epub ahead of print: 11 Aug 2020].
27 Bălănescu A, Bălănescu P, Comănici V, *et al*. Lipid profile pattern in pediatric overweight population with or without NAFLD in relation to IDF criteria for metabolic syndrome: a preliminary study. *Rom J Intern Med* 2018;56:47–54.
28 Ferré P, Foufelle F. Hepatic steatosis: a role for de novo lipogenesis and the transcription factor SREBP-1c. *Diabetes Obes Metab* 2010;12 Suppl 2:83–92.
29 Yan F, Wang Q, Lu M, *et al*. Thyrotropin increases hepatic triglyceride content through upregulation of SREBP-1c activity. *J Hepatol* 2014;61:1358–64.
30 Pawlak M, Lefebvre P, Staels B. Molecular mechanism of PPARα action and its impact on lipid metabolism, inflammation and fibrosis in non-alcoholic fatty liver disease. *J Hepatol* 2015;62:720–33.
31 Montagner A, Polizzi A, Fouché E, *et al*. Liver PPARα is crucial for whole-body fatty acid homeostasis and is protective against NAFLD. *Gut* 2016;65:1202–14.
32 Huang K, Du M, Tan X, *et al*. PARP1-mediated PPARα poly(ADP-ribosyl)ation suppresses fatty acid oxidation in non-alcoholic fatty liver disease. *J Hepatol* 2017;66:962–77.
33 Kaczynski J, Cook T, Urrutia R. Sp1- and Krüppel-like transcription factors. *Genome Biol* 2003;4:206.
34 Black AR, Black JD, Azizkhan-Clifford J. Sp1 and Krüppel-like factor family of transcription factors in cell growth regulation and cancer. *J Cell Physiol* 2001;188:143–60.
35 Tung B, Xia S. Kruppel-like factor 4 (KLF4) and its regulation on mitochondrial homeostasis. *J Stem Cell Res Ther* 2018;8. doi:10.4172/2157-7633.1000436. [Epub ahead of print: 14 Sep 2018].
36 Wang L, Tong X, Gu F, *et al*. The Klf14 transcription factor regulates hepatic gluconeogenesis in mice. *J Biol Chem* 2017;292:21631–42.
37 Haldar SM, Jeyaraj D, Anand P, *et al*. Kruppel-Like factor 15 regulates skeletal muscle lipid flux and exercise adaptation. *Proc Natl Acad Sci U S A* 2012;109:6739–44.
38 Prosdocimo DA, Anand P, Liao X, *et al*. Kruppel-like factor 15 is a critical regulator of cardiac lipid metabolism. *J Biol Chem* 2014;289:5914–24.
39 Sugi K, Hsieh PN, Ilkayeva O, *et al*. Kruppel-like factor 15 is required for the cardiac adaptive response to fasting. *PLoS One* 2018;13:e0192376.
40 Zhang H, Chen Q, Yang M, *et al*. Mouse KLF11 regulates hepatic lipid metabolism. *J Hepatol* 2013;58:763–70.

41 Bechmann LP, Vetter D, Ishida J, *et al*. Post-transcriptional activation of PPAR alpha by KLF6 in hepatic steatosis. *J Hepatol* 2013;58:1000–6.
42 Funnell APW, Maloney CA, Thompson LJ, *et al*. Erythroid Krüppel-like factor directly activates the basic Krüppel-like factor gene in erythroid cells. *Mol Cell Biol* 2007;27:2777–90.
43 Kim MH, Seong JB, Huh J-W, *et al*. Peroxiredoxin 5 ameliorates obesity-induced non-alcoholic fatty liver disease through the regulation of oxidative stress and AMP-activated protein kinase signaling. *Redox Biol* 2020;28:101315.
44 Chen X, Li S, Ke Y, *et al*. Klf16 suppresses human glioma cell proliferation and tumourigenicity by targeting TFAM. *Artif Cells Nanomed Biotechnol* 2018;46:608–15.

Supplementary Materials and Methods

Ethics statement

Human specimens used in this study were taken from patients with cholecystitis who underwent liver biopsy at the First Affiliated Hospital of Guangzhou University of Chinese Medicine. Written informed consent was obtained from each patient included in the study and the study protocol conforms to the ethical guidelines of the 1975 Declaration of Helsinki as reflected in a priori approval by the ethics committees of the First Affiliated Hospital of Guangzhou University of Chinese Medicine (NO. K [2019]082). In the field of animal experiments, all animal care and experiments were conducted in strict accordance with the recommendations of the Guide for the Care and Use of Laboratory Animals of the Ministry of Health (China), and approved by the Ethics Committee of Guangzhou University of Chinese Medicine (20190508002).

Animals and experimental design

Male C57BL/6J mice, C57BL/KsJ mice, *ob/ob* mice and *db/db* mice aged 6-8 weeks were purchased from the Model Animal Research Center of Nanjing University (Nanjing, China). $Klf16^{fl/fl}$ mice were generated by the CRISPR/Cas9 system. The gRNA to mouse Klf16 gene, the donor vector containing 2 loxP sites flanked exon1, and Cas9 mRNA were co-injected into fertilized mouse eggs to generate targeted conditional knockout offspring. F0 founder animals were identified by PCR followed by sequence analysis, and bred with wildtype mice to generate germline transmission F1 founders. F1 founders were genotyped by tail genomic PCR/DNA sequencing and Southern blot examination was performed to further confirm correct genotype.

gRNA target sequence (http://crispor.tefor.net/)

gRNA-A1 (matching forward strand of gene): CGTGTCTCCGCGTCCTTGCCCGG

gRNA-A2 (matching forward strand of gene): GGGTCGGTAGATCCGGGTTACGG

Albumin-Cre mice were provided by Hongbing Zhang (Institute of Basic Medical Sciences, Peking Union Medical College). Hepatic-specific Klf16 knockout mice were generated by crossing $Klf16^{fl/fl}$ mice with Albumin-Cre mice (called $Klf16^{alb-/-}$). Age-matched male littermates $Klf16^{fl/fl}$ mice were used as controls.

Pparα$^{-/-}$ mice were generated by the CRISPR/Cas9 system at Cyagen. The exon 4~6 have been selected as the target site. Briefly, gRNA sequences were designed by the CRISPR design tool (http://crispr.mit.edu) to target upstream and downstream from the coding region exon 4~6, respectively, and then were screened for off-target activity using a Universal CRISPR Activity Assay (UCA) (Biocytogen). Based on a sgRNA activity assay, these gRNAs targeting vectors were selected.

gRNA target sequence:

gRNA1 (matching reverse strand of gene): ATATTACAGGACCTCCACGGGGG

gRNA2 (matching forward strand of gene): TAATACCTTACCTAGTATCGGGG

These gRNA vectors were constructed and confirmed by sequencing, then were transcribed into short RNA by in vitro transcription. Then the Cas9 mRNA, gRNA were co-microinjected into the cytoplasm of 2-cell stage fertilized C57BL/6N eggs. The injected zygotes were transferred into oviducts of ICR surrogate females to generate F0 mice. F0 mice with the expected genotype confirmed by tail genomic DNA PCR and sequencing were mated with C57BL/6N mice to establish germline-transmitted F1 founders.

All mice were housed and maintained on a 12-h-light-dark cycle with a regular unrestricted diet. To establish NAFLD model, mice were fed a high-fat diet (Rodent Diet with 60 Kcal% Fat) ad libitum for 12 weeks without water limitation. To generate alcohol fatty liver models, mice were subjected to NIAAA alcohol model protocol. Briefly, mice were acclimated to a control liquid diet (Bio-Serv, F1259SP) for one day, followed by feeding with a liquid diet containing a gradual increased ethanol concentration from 1-4% (vol/vol) for day 2 to day 5. From day 6, the mice fed a liquid diet containing 5% ethanol for 10 days, and control groups were pair-fed a control diet for 10 days. At day 11, mice were gavaged with a single dose of ethanol (5g/kg, 30% ethanol), while the control groups were gavaged with isocaloric dextrin maltose. All mice were sacrificed 9h after gavage.

Male C57BL/6J mice, *db/db* mice aged 8 weeks or male C57BL/6J mice fed with HFD for 12 weeks were injected i.v. through the tail vein with adeno-associated virus expressing green fluorescent protein (AAV-*egfp*) or adeno-associated virus expressing KLF16(AAV-*Klf16*)(8.45E+12GC/ml). After four weeks of infection,

experiments were conducted. For Pparα overexpression, male Klf16$^{alb-/-}$ on HFD for 12 weeks were injected i.v. through the tail vein with adenovirus expressing green fluorescent protein (Ad-*egfp*) or adenovirus expressing Pparα(Ad-*Pparα*) (1.0×10^9 active viral particles in 200μl saline [54 mmol/l NaCl]). After one week of infection, experiments were conducted. All mice were fasted for 6h before sacrificed. Livers and serum were collected for further analysis. All mice were randomly assigned, and the experimenter was blind to the assignment of the groups and the evaluation of the results. No samples, animals or data, were excluded.

Preparation of recombinant adeno-associated virus (AAV)

To generate KLF16 overexpression adeno-associated virus, the primers sequence containing restriction sites used as follows:

KLF16-SacI-fw, 5'- CGAGCTCGCCACCATGTCGGCGGCCGTGGCGTG-3'

KLF16-EcoRI-rv, 5'- CGGAATTCTCAGGGCAAGGCGGAGCCGGA-3'

AAV2/8-KLF16-P2A-ZsGreen and AAV2/8-ZsGreen were further packaged (DongBio.Co.Ltd, Shenzhen, China) and the final titers for use were 1×10^{12} vector genome (v.g.)/ml. A total amount of $0.5\text{-}1\times10^{11}$ v.g. diluted in 200 μl of PBS was delivered to mice via tail vein injection.

Preparation of expression plasmids and recombinant adenoviruses

The full-length mouse Klf16 gene was amplified by PCR from C57BL/6J mouse liver cDNA, and myc-tagged Klf16 was cloned into pcDNA3.1 (Invitrogen, Carlsbad, CA, USA) using the following PCR primer pairs:

F: 5′-ACGCAGATCGAATTCATGTCGGCGGCCGTGGCGTGTGTGGATTACTT-3′

R: 5′-AAACAAGTTGCTCGAAGTCGACGAGCTCAAGCTTTCAGGGCAAGGCG-3′

Recombinant Adenovirus expressing vectors were purchased from Promega (Madison, WI, USA) and generated as previously described. For Klf16 overexpression, the full-length mouse KLF16 gene was amplified by PCR from the C57BL/6J mouse liver cDNA library and then was subcloned into pAd-Track-CMV vector. The primers sequence as follows:

F:5'-GAATTCATGTCGGCGGCCGTGGCGTGTGTGGATTACTT-3'

R:5'-CAAGCCAGCAGGAGCTGGGCTGGGGACAGGGCTAG -3'

For KLF16 knockdown, short-hairpin RNA (shRNA)-encoding DNA sequences were synthesized by Invitrogen (Carlsbad, CA) and constructed into adenovirus plasmids (pAdTrack-U6 vectors), The primers sequence as follows:

F:5'-AAGCTCCGGCCAAAGCCTATTACAAGTCTTCTCGAGAAGACTTGTAATAGGCTTTGGTTTTTG-3'

R:5'-

GGTACAAAAACCAAAGCCTATTACAAGTCTTCTCGAGAAGACTTGTAATAGGCTTTGGCCGGA-3'

Adenovirus expressing Pparα(Ad-*Pparα*) was kindly provided by prof.Chang lab.

RNA extraction and quantitative (q) real-time PCR

Total RNA was extracted from mouse liver or cells with TRIzol (Takara), and then reverse-transcribed to cDNA with a high-capacity cDNA reverse transcription kit (Applied Biological Materials Inc, Vancouver, Canada). qPCR (PowerUp^{TM} SYBR^{TM} Green Master Mix) was performed by using gene-specific primers and SYBR Green. All gene expression data were normalized to β-actin expression levels. The data was analyzed using the □□CT cycle threshold method, and the mRNA transcription levels of target genes in each group of experiments were expressed as a multiple relative to the control groups. The specific primer sequences are listed in electronic supplementary material (ESM) Table 1.

Western blot analysis

Proteins were extracted from frozen liver samples or cultured hepatocytes in cell lysis buffer, and the total protein concentrations were determined by BSA method. In total, 80-100μg of protein was loaded onto a 10% SDS–polyacrylamide gel, and then separated proteins were transferred to polyvinylidene difluoride membranes. Western blot assays were performed using antibodies specific for rabbit anti-PPARα, rabbit anti-CPT1a (Servicebio, Wuhan, China), rabbit anti-KLF16 (Bioss, Beijing, China), and mouse anti-β-actin (Cwbio, Beijing, China). Antibodies against p-Akt(Ser473), Akt, p-GSK3β, GSK3β were purchased from Cell signaling

Technology.

Luciferase reporter gene assay

HepG2 cells (American Type Culture Collection, Manassas, VA, USA) were cultured in 24-well plates using DMEM Medium containing 10% FBS (Invitrogen). Luciferase reporter genes were then co-transfected into cells, together with the indicated expression plasmids (pcDNA3.1 and pcDNA3.1-Klf16 plasmids, Series of luciferase reporter constructs containing the PPARα gene promoter fragment were kindly provide by prof. Chang), Plasmid containing PPARα gene promoter mutant fragment were constructed by PCR using -1286Luc as a template. The primers used for mutant fragment are F:CTGAGCCGGGGCCCGGGCCT; R:AGGCCCGGGCCCCGGCTCAG). The Ramlila luciferase expression vector pCMV-RL-TK (Promega) was used as an internal control. After 48h, cells were harvested and evaluated for luciferase activity using the Dual Luciferase Reporter Assay System (Promega). Relative luciferase activity was corrected for Renilla luciferase activity of pCMV-RL-TK, and normalized to the activity of the control.

Mitochondrial DNA copy number

The mitochondrial DNA (mtDNA) copy numbers are used as qPCR markers for mitochondrial density. In Brief, total DNA was isolated from mice liver using a Universal Genomic DNA Extraction kit (Tiangen), as described by the manufacturer. Mitochondrial DNA copy number is expressed by the COXII (mitochondrial-encoded gene)/Rps18 ratio. The primer sequences of COX II and Rps18 are presented in (ESM) Table 2.

Histology and immunohistochemistry

For H&E straining, liver tissues were fixed in 10% neutral-buffered formalin, embedded in paraffin, and cut into 7μm sections. For Oil red O staining, liver tissue was frozen in liquid nitrogen and cut into 10μm sections. Sections were stained and analyzed at 100X magnification with Masson's trichrome staining being used to determine collagen deposition.

Assessment of mitochondrial membrane potential

Mitochondrial membrane potential of MPHs was detected using JC-1assay kit (C2006, Beyotime, Shanghai,

China). In Brief, Primary hepatocytes were seeded in 6-well plates and transfected with pcDNA3.1-Klf16 or pcDNA3.1 using lipo3000 according to its manufacturer. After 24h, medium was replaced with OA&PA containing fresh medium for another 24h. MPHs were fixed with 4% paraformaldehyde for 20 minutes and mitochondrial membrane potential was measured according to the manufacturer's instructions and illustrated by fluorescence microscopy imaging (Leica Microsystems Ltd., Wetzlar, Germany).

Supplementary Tables

Table 1. Primer information for gene amplification

Primer	Sequences
KLF16(m)	F1: GTGTACCAAGCGGTTCACC
	R1: CAGGTCGTCGCAGGAGTTC
PPARα(m)	F1:AACATCGAGTGTCGAATATGTGG
	R1:CCGAATAGTTCGCCGAAAGAA
MgII(m)	F1: AGGCGAACTCCACAGAATGTT
	R1: ACAAAAGAGGTACTGTCCGTCT
HSL(m)	F1: GATTTACGCACGATGACACAGT
	R1: ACCTGCAAAGACATTAGACAGC
Atgl(m)	F1: ATGTTCCCGAGGGAGACCAA
	R1: GAGGCTCCGTAGATGTGAGTG
Acadvl(m)	F1: ACTACTGTGCTTCAGGGACAA
	R1: GCAAAGGACTTCGATTCTGCC
Acadl(m)	F1: TTTCCTCGGAGCATGACATTTT
	R1: GCCAGCTTTTTCCCAGACCT
Acads(m)	F1: GACTGGCGACGGTTACACA
	R1: GGCAAAGTCACGGCATGTC
Cpt2(m)	F1: CAGCACAGCATCGTACCCA
	R1: TCCCAATGCCGTTCTCAAAA
Cpt1a(m)	F1: TGGCATCATCACTGGTGTGTT

	R1: TCTAGGGTCCGATTGATCTTTG
Cpt1b(m)	F1: GACTTCCGGCTTAGTCGGG
	R1: GAATAAGGCGTTTCTTCCAGGA
Fabp3(m)	F1: ACCTGGAAGCTAGTGGACAG
	R1: TGATGGTAGTAGGCTTGGTCAT
β-actin(m)	F1: ATGACCCAAGCCGAGAAGG
	R1: CGGCCAAGTCTTAGAGTTGTTG
TNFα(m)	F1: CAGGCGGTGCCTATGTCTC
	R1: CGATCACCCCGAAGTTCAGTAG
IL-6(m)	F1:CTGCAAGAGACTTCCATCCAG
	R1: GTGGTATAGACAGGTCTGTTGG
IL-10(m)	F1: TTACTGACTGGCATGAGGATCA
	R1: GCAGCTCTAGGAGCATGTGG
IL-1beta(m)	F1: GAAATGCCACCTTTTGACAGTG
	R1: TGGATGCTCTCATCAGGACAG
KLF16(h)	F1: CAAGTCCTCGCACCTAAAGTC
	R1: AGCGGGCGAACTTCTTGTC
PPARα(h)	F1: ATGGTGGACACGGAAAGCC
	R1: GATGGATTGCGAAATCTCTTGG
GAPDH(h)	F1: GGAGCGAGATCCCTCCAAAAT
	R1: GGCTGTTGTCATACTTCTCATGG

Supplementary Figures

Figure Legend

Figure1. Hepatic KLF16 expression is decreased in hepatic steatosis

(A) KLF16 mRNA levels in C57BL/6J mice subjected to fasting and refeeding cycle.

(B) QPCR analyses indicated that KLF16 expression was decreased in NALFD patients (n=38) than in controls (n=28).

(C) OA&PA treatment decreased KLF16 mRNA levels in mice primary hepatocytes.

Comparable results obtained in three independent experiments.

Data are means ± SEM; n=8 mice/group. $*p < 0.05$, $**p < 0.01$, $***p < 0.001$

Figure2. Hepatic KLF16 deficiency worsens hepatic steatosis and increases insulin resistance

(A) QPCR data indicated a deletion of KLF16 in the liver, rather than other tissues.

(B) KLF16 deficiency increased the ratio of liver/body weight in chow diet mice.

(C) KLF16 knockout increased serum and hepatic TGs levels of mice fed on chow diet, while has no effects on the TC levels.

(D) KLF16 deletion increased the fasting blood glucose levels and insulin levels of chow diet mice.

(E) KLF16 deficiency impaired pyruvate tolerance of mice on chow diet, repeated measure two way ANOVA was used to analysis the difference of two curves.

(F) The hepatic Pepck, G6pase mRNA levels were upregulated due to KLF16 deficiency in chow diet mice.

(G&H) KLF16 deletion impaired mitochondrial biogenesis (G) and altered mitochondrial ultrastructure (H).

(I) KLF16 deletion increased hepatic ROS overproduction in chow diet mice.

(J) KLF16 deletion suppressed genes involved in anti-oxidant response.

(K) KLF16 deficiency stimulates hepatic inflammatory genes in chow diet mice.

Comparable results obtained in three independent experiments.

Data are means ± SEM; n=8 mice/group. $*p < 0.05$, $**p < 0.01$, $***p < 0.001$

Figure3. KLF16 overexpression alleviates hepatic steatosis in *db/db* mice

(A) QPCR data indicated KLF16 mRNA levels were not altered in other tissues in *db/db* mice.

(B) KLF16 overexpression does not alter body weight of *db/db* mice.

(C) KLF16 overexpression reduced serum and hepatic TGs levels, while has no effects on the TC levels in *db/db* mice.

(D) KLF16 overexpression decreased fasting blood glucose and insulin levels in *db/db* mice.

(E) KLF16 overexpression improved pyruvate tolerance of *db/db* mice, repeated measure two way ANOVA was used to analysis the difference of two curves.

(F) The Pepck, G6pase mRNA levels were decreased in *db/db* mice after KLF16 overexpression.

(G) KLF16 overexpression reduced serum ALT and AST levels in *db/db* mice.

(H&I) KLF16 overexpression in *db/db* mice improved mitochondrial biogenesis (H) and mitochondrial ultrastructure (I).

(J) KLF16 overexpression decreased hepatic ROS overproduction in *db/db* mice.

(K) KLF16 overexpression up-regulates genes involved in anti-oxidant response in *db/db* mice.

(L) KLF16 overexpression decreased hepatic inflammatory genes in *db/db* mice.

Comparable results obtained in three independent experiments.

Data are means ± SEM; n=8 mice/group. $*p < 0.05$, $**p < 0.01$, $***p < 0.001$

Figure4. KLF16 overexpression attenuated hepatic steatosis in HFD mice

(A) QPCR data indicated KLF16 mRNA levels were unchanged in other tissues in HFD mice.

(B) KLF16 overexpression does not alter body weight of HFD mice.

(C) KLF16 overexpression reduced the ratio of liver/body weight in HFD mice.

(D) KLF16 overexpression reduced serum and hepatic TGs levels of HFD mice, while has no effect on TC content.

(E) KLF16 overexpression reduced serum ALT and AST levels in HFD mice.

(F) KLF16 overexpression decreased fasting blood glucose and insulin levels in HFD mice.

(G) KLF16 overexpression reduced the expression of hepatic Pepck and G6pase in HFD mice.

(H) KLF16 overexpression decreased hepatic inflammatory genes in HFD mice.

Comparable results obtained in three independent experiments.

Data are means ± SEM; n=8 mice/group. $*p < 0.05$, $**p < 0.01$, $***p < 0.001$

Figure5. KLF16 affects lipid deposition in mice primary hepatocytes

(A) TG levels of mice primary hepatocytes infected with ad-*gfp* or ad-*Klf16* treated with DMSO or OA&PA for 24h. (B) TG levels of mice primary hepatocytes infected with ad-*shLuci* or ad-*shKlf16* treated with DMSO or OA&PA for 24h.

Comparable results obtained in three independent experiments.

Data are means ± SEM; n=6/group. $*p < 0.05$, $**p < 0.01$, $***p < 0.001$

Figure6. PPARα overexpression attenuated KLF16 deficiency-induced hepatic steatosis

(A) QPCR and WB data indicated PPARα overexpression in mice primary hepatocytes and livers.

(B) QPCR data indicated unchanged PPARα expression in other tissues of $KLF16^{alb-/-}$ mice after ad-PPARα infection.

(C&D) PPARα overexpression reduced body weight (C) and the ratio of liver/body weight (D) in $KLF16^{alb-/-}$ mice fed on HFD.

(E) PPARα overexpression increased mitochondrial biogenesis (*left panel*) and mitochondrial ultrastructure (*right panel*).

(F&G) PPARα overexpression decreased hepatic ROS overproduction (F) and inflammatory genes (G) in HFD $KLF16^{alb-/-}$ mice.

(H) PPARα overexpression reduced serum ALT and AST levels in HFD $KLF16^{alb-/-}$ mice.

(I) PPARα overexpression decreased fasting blood glucose and insulin levels of HFD $KLF16^{alb-/-}$ mice.

Comparable results obtained in three independent experiments.

Data are means ± SEM; n=8 mice/group. *$p < 0.05$, **$p < 0.01$, ***$p < 0.001$

Figure7. KLF16 affects ROS production in mice primary hepatocytes

(A) KLF16 overexpression effectively decreased OA&PA-induced ROS over-production in mice primary hepatocytes.

(B) KLF16 deletion aggravated OA&PA-induced ROS over-production in mice primary hepatocytes.

Comparable results obtained in three independent experiments.

Figure8. Hepatic KLF16 deletion increases mice sensitivity to ethanol feeding

(A) Ethanol feeding decreased hepatic KLF16 protein levels.

(B) KLF16 deletion aggravated ethanol feeding-induced elevation of serum ALT and AST levels.

(C) KLF16 deletion aggravated hepatic inflammatory genes after ethanol feeding.

(D) The mitochondrial ultrastructure was changed in $KLF16^{alb-/-}$ mice after ethanol feeding.

(E) KLF16 deletion increased hepatic ROS generation in $KLF16^{alb-/-}$ mice after ethanol feeding.

Comparable results obtained in three independent experiments.

Data are means ± SEM; n=8 mice/group. *$p < 0.05$, **$p < 0.01$, ***$p < 0.001$

Figure9. KLF16 has no effects on SREBP-1c expression

(A) KLF16 overexpression did not changed the protein levels of SREBP-1c both in cytoplasm and nucleus of MPHs.

Comparable results obtained in three independent experiments.

Figure10. The effect of KLF16 on apoptosis.

(A) KLF16 overexpression inhibits apoptosis in mice primary hepatocytes, as shown by the mitochondrial membrane potential changes of mice primary hepatocytes transfected with pcDNA3.1+KLF16 or pcDNA3.1 as control, followed by the OA&PA exposure for 24h.

(B) qPCR analysis of key genes involved in apoptosis in the liver of *db/db* and DIO mice infected with aav-*egfp* or aav-*Klf16*, as well as the liver of $Klf^{alb-/-}$ mice and $Klf16^{fl/fl}$ mice.

Comparable results obtained in three independent experiments.

Data are means ± SEM; $*p < 0.05$, $**p < 0.01$

Supplementary Figure 1

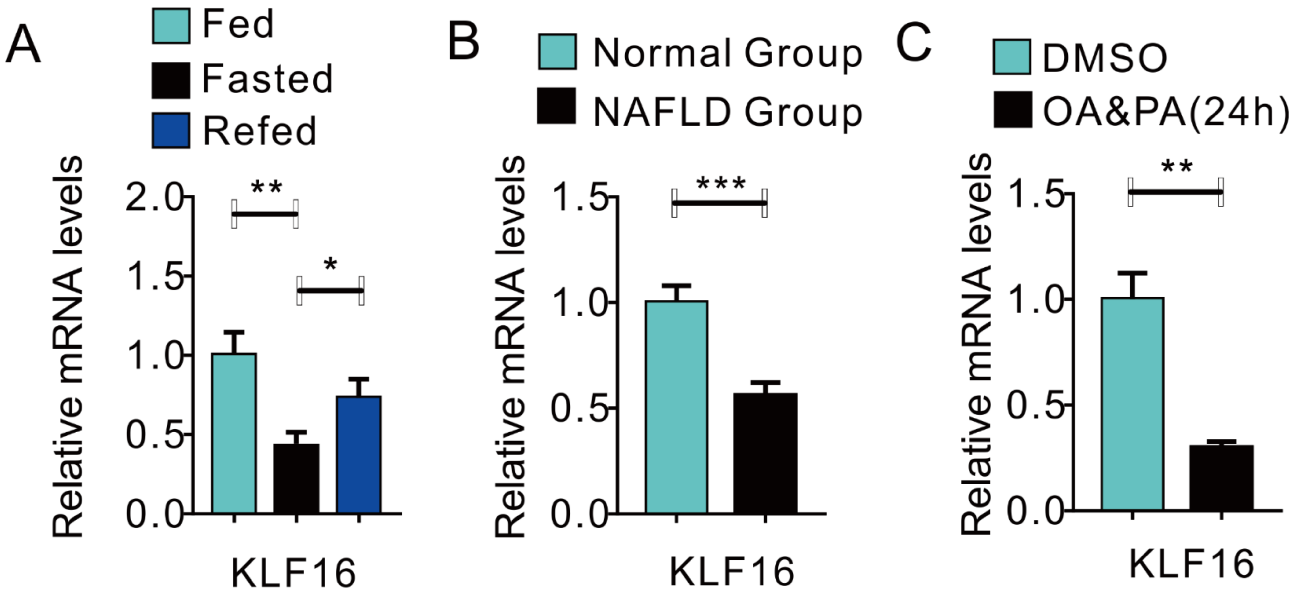

Supplementary Figure 2

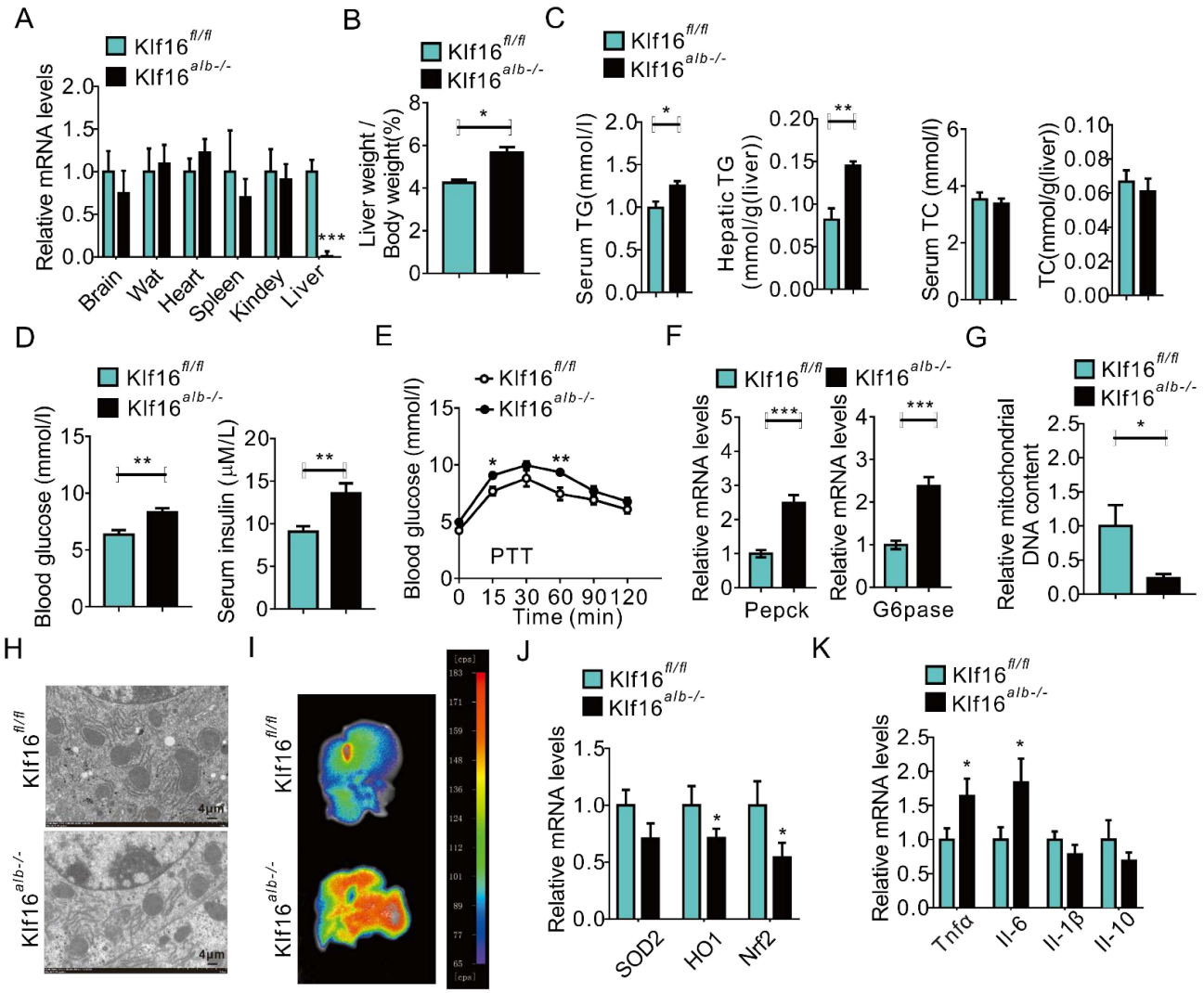

Supplementary Figure 3

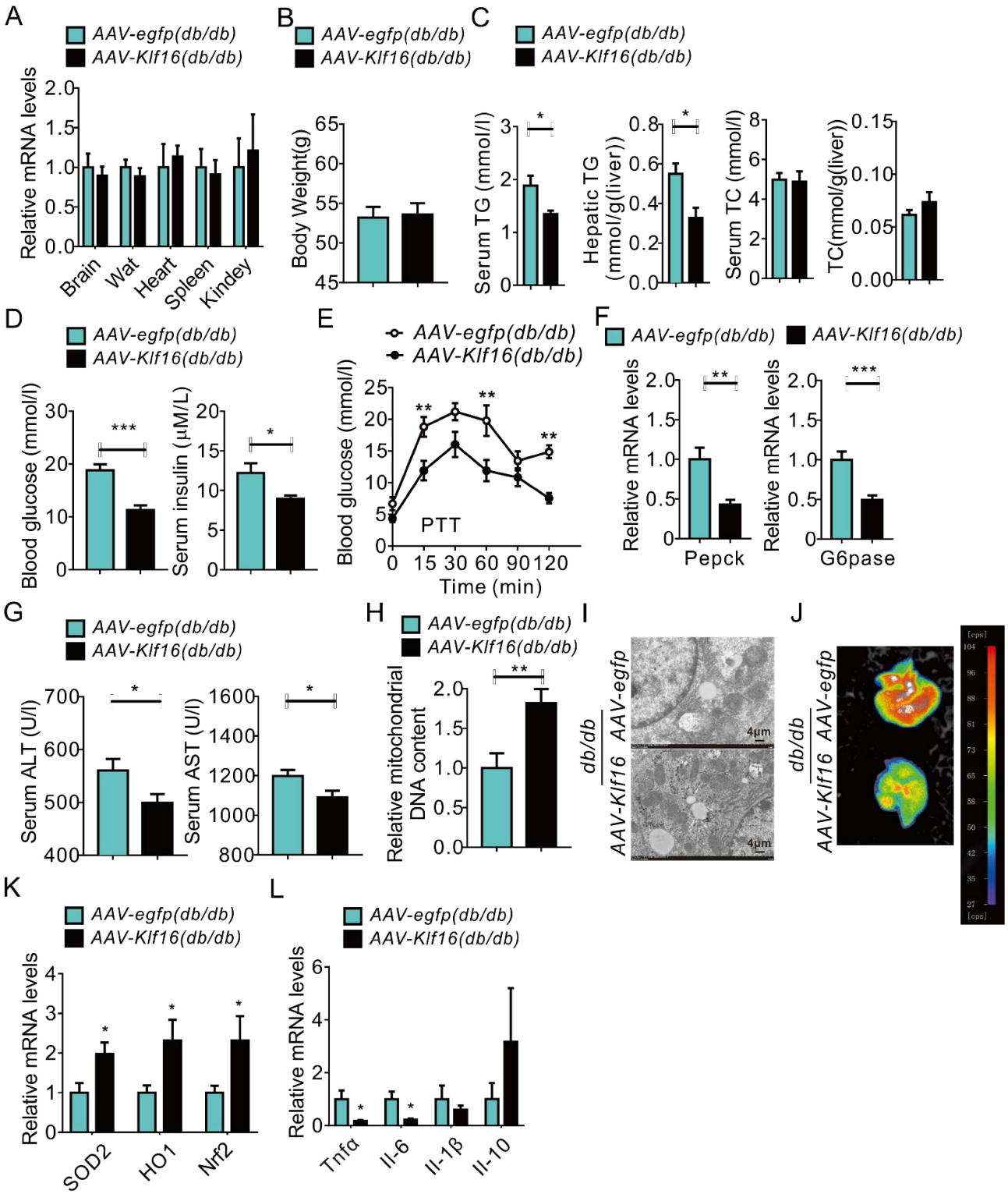

Supplementary Figure 4

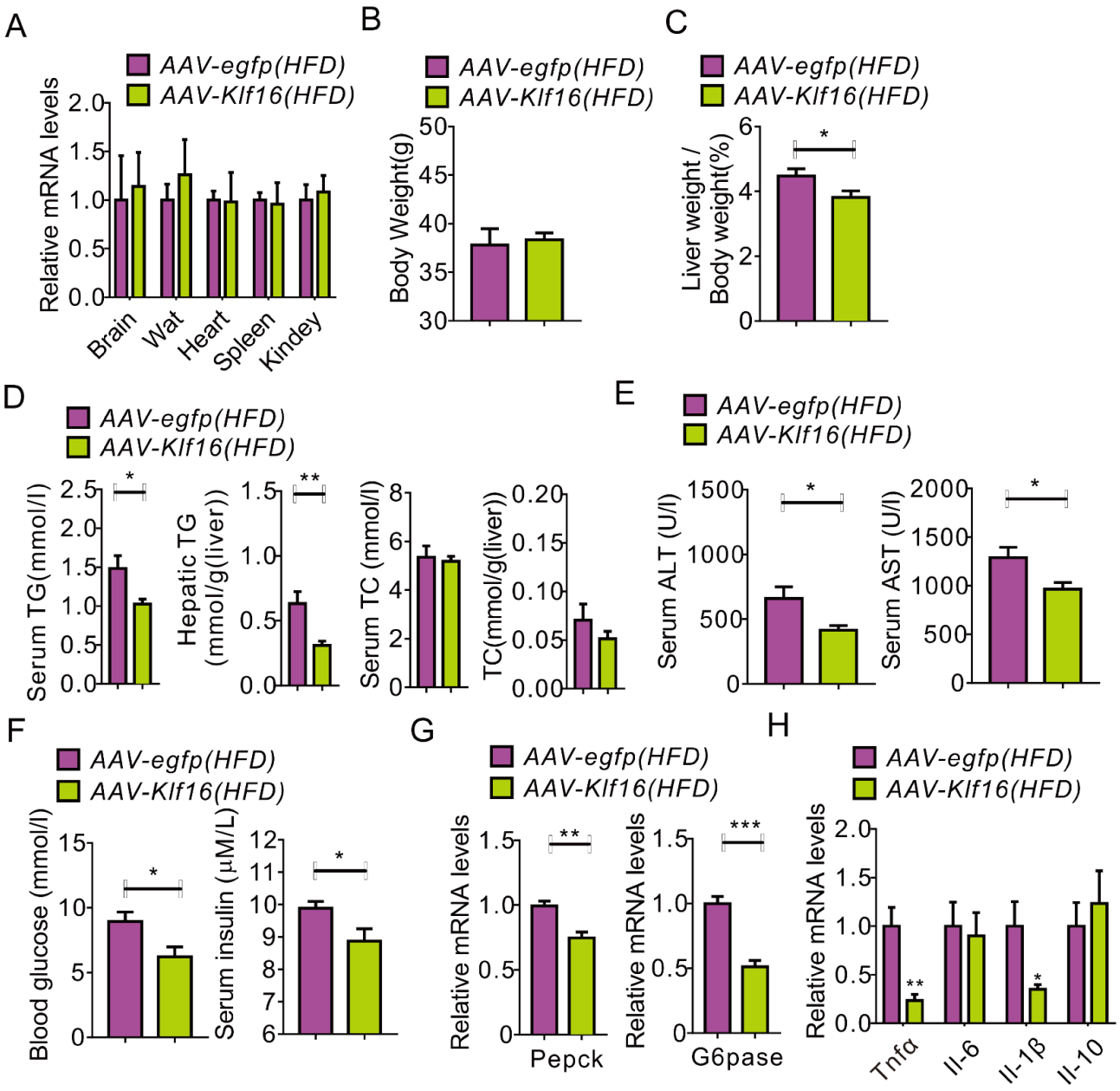

Supplementary Figure 5

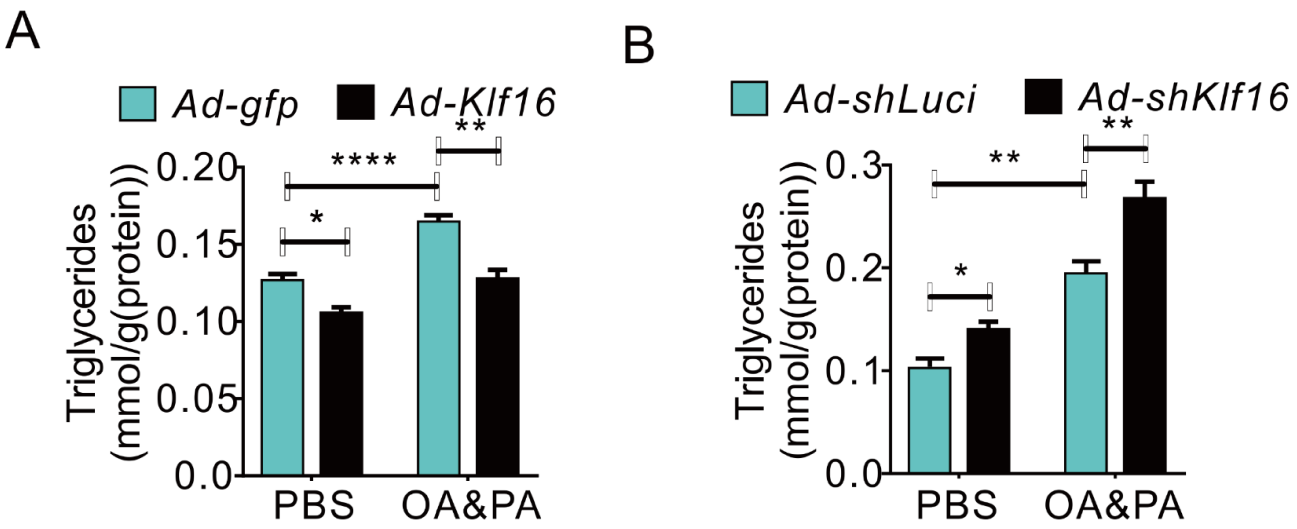

Supplementary Figure 6

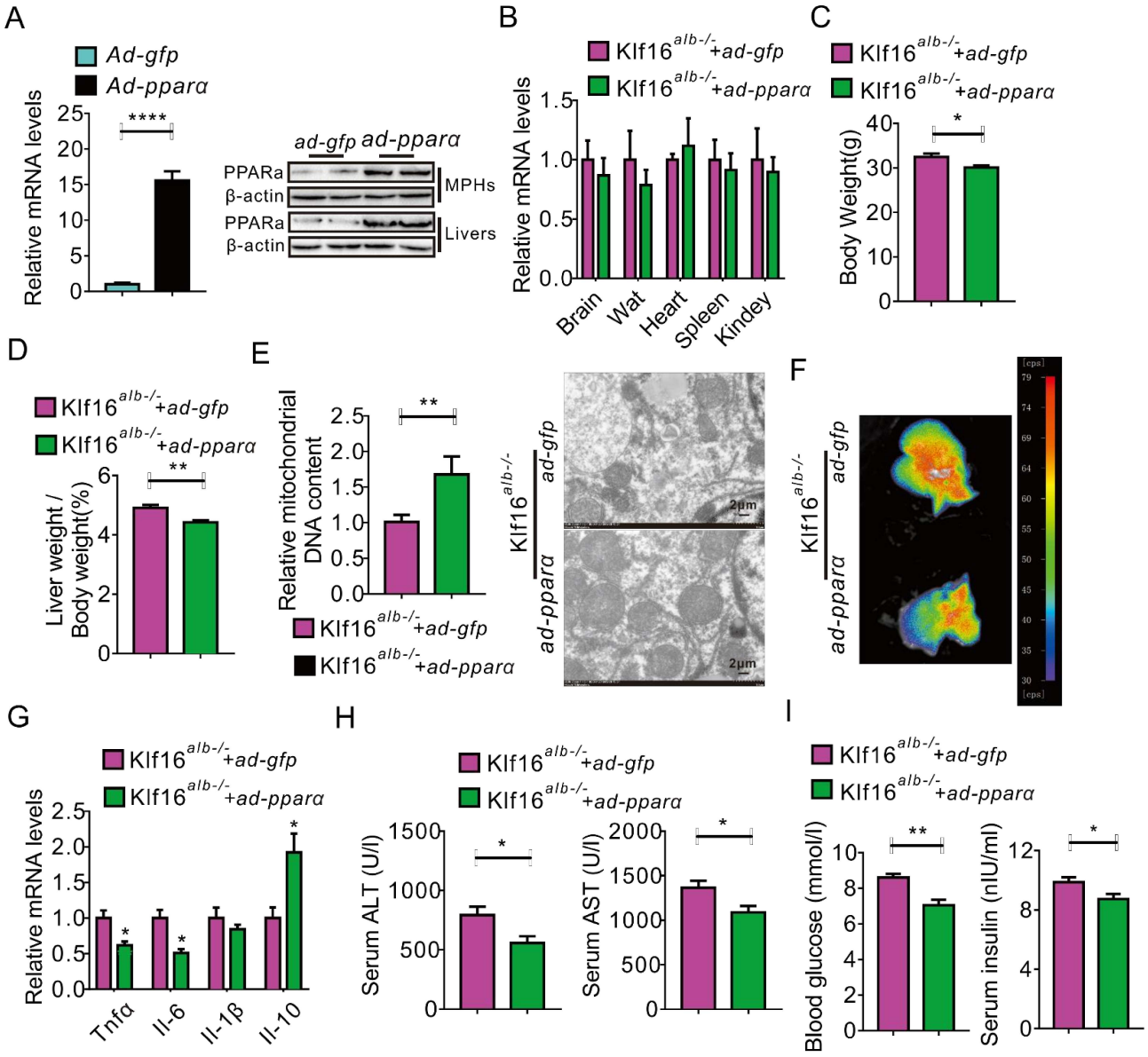

Supplementary Figure 7

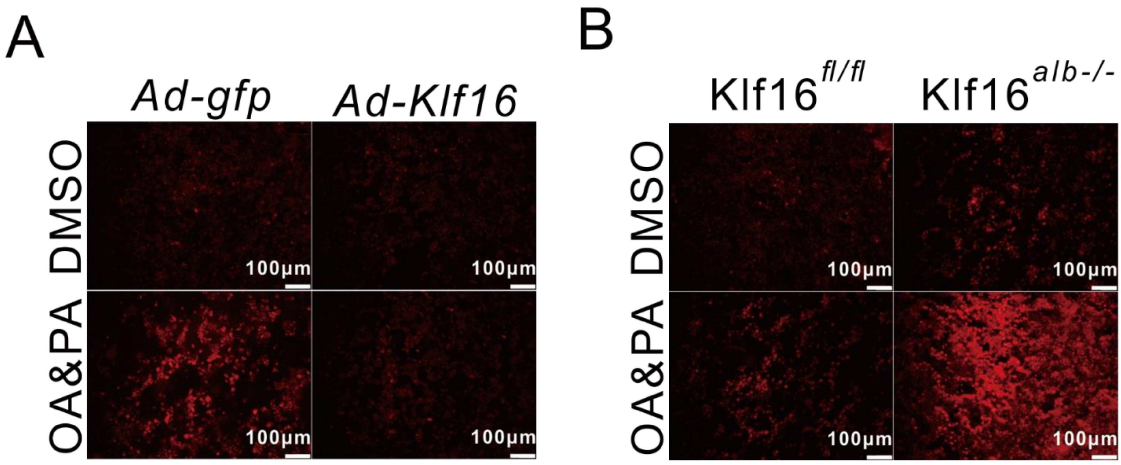

Supplementary Figure 8

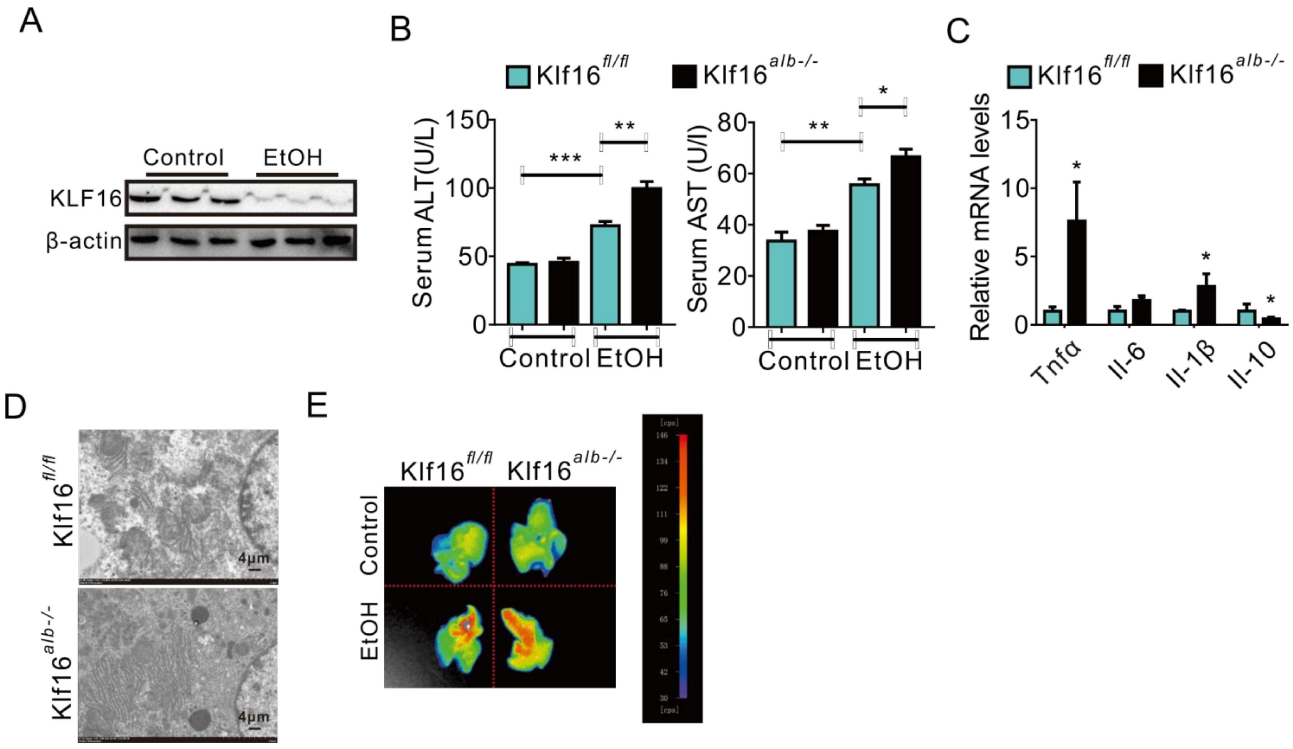

Supplementary Figure 9

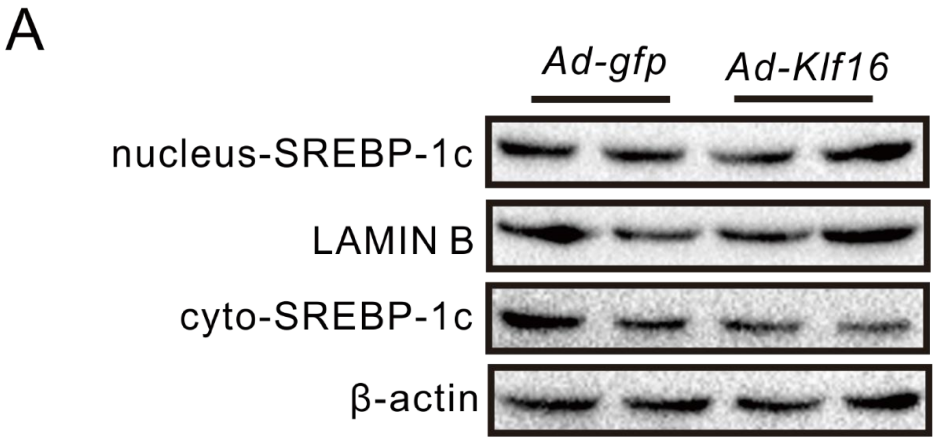

Supplementary Figure 10